BRNO UNIVERSITY OF TECHNOLOGY

VYSOKÉ UČENÍ TECHNICKÉ V BRNĚ

FACULTY OF MECHANICAL ENGINEERING

FAKULTA STROJNÍHO INŽENÝRSTVÍ

INSTITUTE OF MANUFACTURING TECHNOLOGY

ÚSTAV STROJÍRENSKÉ TECHNOLOGIE

SIMULATION OF HEADLIGHT COVER LENS DE-ICING AND ITS APPLICATION IN AUTOMOTIVE INDUSTRY

SIMULACE ODMRAZOVÁNÍ KRYCÍHO SKLA SVĚTLOMETU A JEHO APLIKACE V AUTOMOBILOVÉM PRŮMYSLU

MASTER'S THESIS

DIPLOMOVÁ PRÁCE

AUTHOR — Bc. Jan Magdon

AUTOR PRÁCE

SUPERVISOR — Ing. Jan Boháček, Ph.D.

VEDOUCÍ PRÁCE

BRNO 2021

BRNO UNIVERSITY OF TECHNOLOGY
FACULTY OF MECHANICAL ENGINEERING

Assignment Master's Thesis

Institut:	Institute of Manufacturing Technology
Student:	**Bc. Jan Magdon**
Degree programm:	Mechanical Engineering
Branch:	Production of Automotive and Technical Lights
Supervisor:	**Ing. Jan Boháček, Ph.D.**
Academic year:	2020/21

As provided for by the Act No. 111/98 Coll. on higher education institutions and the BUT Study and Examination Regulations, the director of the Institute hereby assigns the following topic of Master's Thesis:

Simulation of headlight cover lens de–icing and its application in automotive industry

Brief Description:

Technology of automotive lightning is advancing by leaps and bounds every year. Obsolete light sources like halogen and xenon lightbulbs are being replaced by LED (Light – Emitting – Diode) technology. The portion of the converted supplied electrical energy into waste heat is high for all mentioned sources, but each source has specific parameters, and thus creates different conditions inside the headlamp. The heat emission of a halogen bulb, same as LEDs, accounts from 80 % to 90 % of the total performance. While a halogen bulb is one of the incandescent light sources that heats its surroundings, LEDs are cold sources of light emission that do not heat up the surroundings. At the same time, LEDs are sensitive devices prone to damage by high temperatures, therefore coolers or fans are connected to them, which dissipate generated heat.

Especially in cold climates, an ice layer may form on the outer parts of the headlamps. The ice layer must be removed as soon as possible to make the vehicle operational. If LED sources are used, there is not enough heat and de–icing would be time–consuming, therefore it is necessary to attach an additional heat source to the headlamp system to speed up the de–icing process. These additional sources must be affordable and efficient, such as heating elements that convert electrical energy into heat.

As LED technology belongs to the range of younger technologies, to solve the problems of headlamps de–icing, it is necessary to develop new numerical models that correspond to the reality.

The aim of this diploma thesis is to develop a numerical model for application of de–icing of the headlamp cover lens. The parameters will be altered in the simulations; their influence on the computational time, computational stability, degree of convergence and others will be then investigated.

Master's Thesis goals:

– Development of the de–icing model in fluid simulations.
– Testing individual parameters of the de–icing model.
– Optimalization for a stable solution with short computational time.
– Use in car headlamps.

Recommended bibliography:

JANSSON, A. De-icing and ice prevention of automotive headlamps and tail lamps. Master's thesis, KTH Industrial Engineering and Management, Stockholm, 2014.

INCROPERA, F. P. and D. P. DEWITT. Fundamentals of Heat and Mass Transfer, New York: J. Wiley, 2002.

FERZIGER, J. H., M. PERIC. Computational Methods for Fluid Dynamic. Third Edition, Springer, Berlin, 2002.

BRUNBERG, J., M. ASPELIN. CFD Modelling of Headlamp Condensation. Master's thesis, Chalmers University of Technology, Göteborg, 2011.

Deadline for submission Master's Thesis is given by the Schedule of the Academic year 2020/21

In Brno,

L. S.

doc. Ing. Petr Blecha, Ph.D. Director of the Institute	doc. Ing. Jaroslav Katolický, Ph.D. FME dean

ABSCRACT

The thesis is written in cooperation with Hella GmbH & Co. KGaA and will engage in research in headlamp de-icing area. The aim is to create a numerical simulation model which is able to predict the course of de-icing process as well as revealing shortcomings and optimize design of the headlamp with respect to required functionality. Variable parameters are tested on the simulation model, the aim of the thesis is to find the optimal conditions that will ensure valid simulation results while saving computational time.

Key words

Simcenter Star CCM+, de-icing, headlamp, Computational Fluid Dynamics, numerical simulation, heat transfer

ABSTRAKT

Práce je psána ve spolupráci s Hella GmbH & Co. KGaA a zabývá se výzkumem v oblasti odmrazování světlometu. Jejím cílem je vytvoření numerického simulačního modelu, který dokáže předpovídat průběh odmrazování, může odhalit nedostatky při návrhu světlometu a optimalizovat design světlometu dle funkčních požadavků. Na simulačním modelu jsou testovány proměnlivé parametry, výsledkem práce je nalezení optimálních podmínek, které zajistí validní výsledky simulace při současné úspoře výpočetního času.

Klíčová slova

Simcenter Star CCM+, odmrazování, světlomet, Computational Fluid Dynamics, numerická simulace, přenos tepla

BIBLIOGRAPHIC CITATION / BIBLIOGRAFICKÁ CITACE

MAGDON, Jan. *Simulace odmrazování krycího skla světlometu a jeho aplikace v automobilovém průmyslu.* Brno, 2021. Dostupné také z: https://www.vutbr.cz/studenti/zav-prace/detail/129583. Diplomová práce. Vysoké učení technické v Brně, Fakulta strojního inženýrství, Ústav strojírenské technologie. Vedoucí práce Jan Boháček.

NOTICE OF COPYRIGHT PROTECTION

OZNÁMENÍ O OCHRANĚ AUTORSKÝCH PRÁV

AFFIDAVIT

I hereby affirm that this master's thesis on theme **Simulation of headlight cover lens de-icing and its application in automotive industry** represents my own written work and that I have used no sources and aids other than those indicated. All passages quoted from publications or paraphrased from these sources are properly cited and attributed in attachment of this master's thesis.

PROHLÁŠENÍ

Prohlašuji, že jsem diplomovou práci na téma **Simulace odmrazování krycího skla světlometu a jeho aplikace v automobilovém průmyslu** vypracoval samostatně s použitím odborné literatury a pramenů, uvedených na seznamu, který tvoří přílohu této práce.

Date/Datum

Bc. Jan Magdon

ACKNOWLEDGMENTS

I would first like to thank my thesis supervisor Dr. Michal Matejka from Hella GmbH & Co. KGaA. He was always open whenever I ran into a trouble spot or had a question about my research or writing and steered me in the right the direction.

I would also like to acknowledge supervisor Ing. Jan Boháček, Ph.D from Brno University of Technology, without his help the thesis could not have been successfully conducted.

Finally, I must express my very profound gratitude to my parents for providing me with unfailing support and continuous encouragement throughout my years of study. Thank you.

PODĚKOVÁNÍ

Nejprve bych chtěl poděkovat vedoucímu mé práce Dr. Michalu Matejkovi ze společnosti Hella GmbH & Co. KGaA. Vždy byl otevřený každému dotazu a kdykoli jsem narazil na problémové místo nebo měl otázku ohledně mého výzkumu nebo psaní, nasměroval mě správným směrem.

Rovněž bych rád poděkoval vedoucímu Ing. Janu Boháčkovi, Ph.D na VUT v Brně, bez jeho pomoci nemohla být práce úspěšně sepsána.

Na závěr musím vyjádřit svou hlubokou vděčnost rodičům za to, že mi během let studia poskytovali neustálou podporu a povzbuzení. Děkuji.

TABLE OF CONTENTS

INTRODUCTION

Technology of automotive lighting is advancing by leaps and bounds every year. Obsolete light sources like halogen and xenon lightbulbs are being replaced by LED (**L**ight - **E**mitting – **D**iode) technology. The portion of the converted supplied electrical energy into waste heat is high for all mentioned sources, but each source has specific parameters, and thus creates different conditions inside the headlamp. The heat emission of a halogen bulb is from 85% to 90%, for LEDs accounts from 60% to 65% of the total performance. While a halogen bulb is one of the incandescent light sources that significantly heats its surroundings, LEDs are cold sources with spread out light emission and heat up the surroundings in smaller scale. At the same time, LEDs are sensitive devices prone to damage by high temperatures, therefore coolers or fans are connected to them, which dissipate generated heat.

Especially in cold climates, ice layer may form on the outer parts of the headlamps. Ice layer must be removed as soon as possible to make the vehicle operational. If LED sources are used, there is not enough heat and de-icing would be time-consuming (or might not occur at all), therefore it is necessary to attach an additional heat source to the headlamp system to speed up the de-icing process. These additional sources must be affordable and efficient, such as heating elements that convert electrical energy into heat.

As LED technology belongs to the range of younger technologies, to solve the problems of headlamps de-icing, it is necessary to develop new numerical models that correspond to reality. The aim of this master’s thesis is to develop a numerical model for application of de-icing of the headlamp cover lens. The parameters will be altered in the simulations; their influence on the computational time, computational stability, degree of convergence and others will then be investigated.

THEORETICAL PART

1 LIGHT SOURCES

Headlamps are car parts which are being constantly innovated and thus significantly affect the look of the car. Evolution of headlamp is powered by continual development of new lighting technologies, because in every headlamp light source can be found and for these components, there are very strict requirements, high quality and safety standards must be observed. Halogen, xenon, and LED technologies are the best-known representatives of headlamp light sources [1].

1.1 Halogen

Halogens are still highly represented light sources used in present-day cars. The first time it was heard about halogen headlamps was in 1962, when they were introduced in Europe. Later, halogen technology was spread to the United States in 1979 [1; 2].

- How it works

Halogen bulbs belong to the category of incandescent light sources, that means they consist of filament made from thermally high resistant material (most often from tungsten), which begins to glow in visible spectrum when electrical energy goes through it. The difference from normal incandescent bulb is the size. Halogen bulbs are smaller than normal incandescent bulbs with the similar wattage. Moreover, halogen gas is used as shielding gas instead of vacuum in normal incandescent bulb. Due to halogen gas presence, degradation processes are reduced, the filament lasts for longer time and there is also less darkening. Halogen gas increases service life of the bulb and it allows higher service temperatures without filament burning out. The consequence of this effect is the higher temperature and light with higher luminous intensity [3; 4; 5; 6].

- Advantages

Simple manipulation: Easy to install or replace, it is only needed to unscrew defective bulb and then screw the new one on. Easy replacement and costs are one of the reasons why halogen bulbs are still widespread and popular [1; 2; 5].

Price: Halogen bulbs are cheaper than other mentioned light sources. Further savings are associated with service costs as halogen bulb may be replaced easily by oneself [1; 2; 5].

Light regulation: Halogen bulbs are able to generate light of different intensity; therefore, they may be used as multifunctional light source (high/low beam, specific weather situations) [1; 2; 5].

- Disadvantages

Temperature: Halogen bulbs are very hot and produce the most heat out of the other mentioned light sources. Heat is generated due to incandescence which produces light but also significant amount of heat [1; 2; 5].

Efficiency: Halogen light bulbs are not very energy efficient. The problem once again lies in incandescence as a lot of energy is lost in the heat production; even though, it is only employed for light [1; 2; 5].

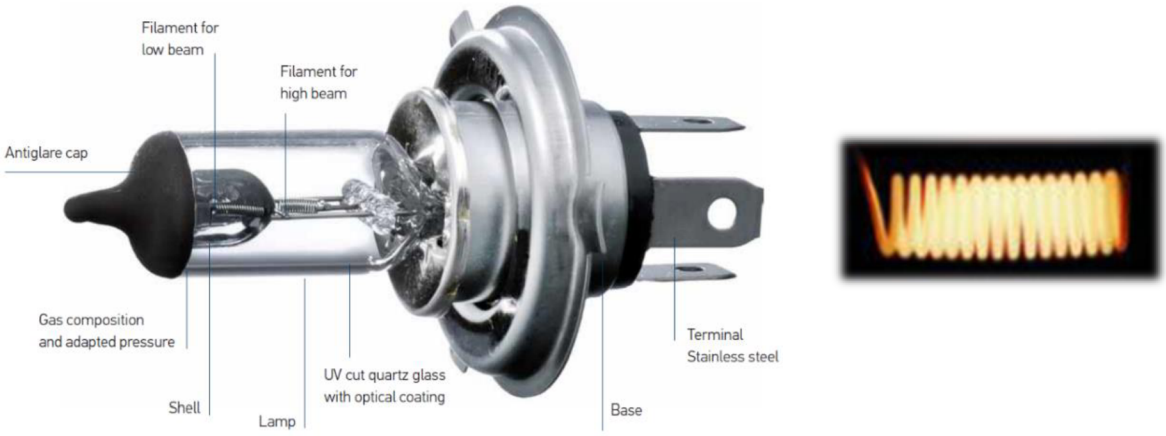

Figure 1.1. Scheme halogen bulb used in headlamp and burning filament [3; 4]

1.2 Xenon

Xenon light sources are also known as HID or xenon HID bulbs. The HID abbreviation stands for High Intensity Discharge and the light is produced by an electric arc. Due to high intensity discharge xenon lights consume less energy and produce light with higher luminous intensity than halogen bulbs. Xenon lights were first used in 1991 by BMW and later they were spread to other vehicles as they offer some advantages over halogen bulbs [1; 2].

- How it works

Xenon bulbs are more complicated than halogen bulbs. Moreover, they work on a different principle. When electrical energy is supplied, high voltage spark (23 000 V) ionizes the xenon gas inside the tube and energy starts to flow through it. The current inside the tube gradually rises and this results in temperature increasing. There is no filament in the bulb, there are only metallic salts. When the temperature is sufficient, metallic salts melt and evaporate. This process takes a few seconds (gasses need to reach their operating temperature), evaporated salts increase the current flow as well (due to lower resistance between electrodes) and xenon bulb reaches the maximum performance. Ignition process consumes a lot of energy but once a xenon bulb reaches the maximum performance, only small amount of energy (85 W) is needed for further flow [3; 4; 5; 7].

- Advantages

Brightness: Xenon bulbs produce the light with higher luminous intensity in comparison to the other mentioned light sources (LED and halogen) [1; 2; 5].

Luminous range: Xenon bulbs are able to shine further and wider; therefore, the light is able to cover larger area and provides perfect visibility [1; 2; 5].

Service life: Xenon bulbs last more than twice as long as halogen lamps; however, they are outperformed by LED with lifespan approximately 5 times longer [1; 2; 5].

Efficiency: Much more energy is consumed during the ignition compared to halogen lamps; however, ignition takes only short time, in the long scale, xenon bulbs are more efficient than halogen bulbs; however, still less efficient than LED [1; 2; 5].

- Disadvantages

Price: Xenon bulbs prices are in the middle; they are more expensive than halogen bulbs and cheaper than LED. Regarding price, it is important to take lifespan into consideration, xenon bulbs need to get changed more often than LED and this fact makes the price of xenon bulb higher than LED price [1; 2; 5].

Strong glare: Due to its strong glare, xenon may blind oncoming drivers, especially when the headlamp is polluted and scatters emitting light (additive systems for headlamp cleaning should be used) [1; 2; 5].

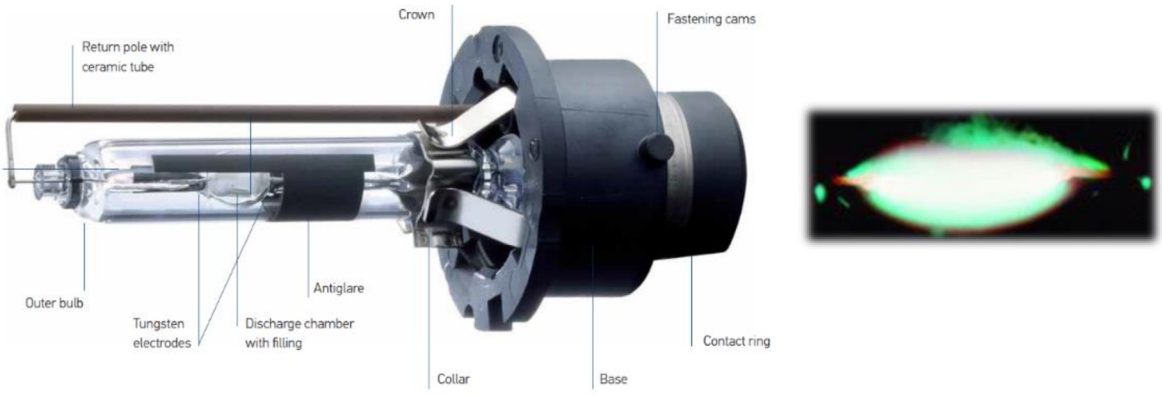

Figure. 1.2. Scheme of a xenon bulb used in headlamp and burning arc [3; 4]

1.3 LED – Light Emitting Diodes

LEDs has existed for decades, firstly red diodes were discovered, later the development shifted to white LEDs, which have many utilizations, one of them is light source for headlamps. LEDs consume relatively small amount of energy and stay at lower temperatures when working (in comparison to other mentioned light sources). Even if working temperatures are small, LED requires cooling, higher temperatures causes LEDs light output degradation and significantly decrease service life (service life is time after illuminating power decreases on the half of its initial value). Single chip LEDs provides relatively a small light output; therefore, sets consisting of many LED chips are also made [1; 2; 8; 9].

LED sources produce light with luminous intensity between halogen bulbs and xenon bulbs. Important advantage over xenon bulbs is less glare and the possibility to produce special shape of light, owing to many individual LEDs. According to the forecast, LED headlamps will make up over 70% of the world´s market by the year 2030 [1; 2].

- How it works

LED shines due to the electroluminescence phenomenon, which was first observed in 1907. Diode is an electronic component which allows the current to flow in one direction. It consists of semiconductor materials. When two semiconductors materials are joined together, with one positively loaded (missing electron = “holes”) and the second one negatively loaded (electrons reside), they create a diode. When electrical current flows through the diode, electrons from the negative semiconductor flow to the positive one, then fall into the hole and sit on the lower energy level. The difference in electron energy is released as photon and light is emitted. The colour of emitted light depends on semiconductor materials and the shape of diodes. Red, green and yellow colours are easy to create. However, it took a long time to develop LEDs producing white light [1; 2; 9].

- Thermal management

Although LEDs are cold sources, they heat up due to light creation process and heat represents about 65% converted electrical energy, the remaining 35% represents light radiation, there is practically no UV (ultra-violet) or IR (infra-red) radiation. The density of heat energy is enormous and could damage heat sensitive diodes and chips. Furthermore, light parameters are dependent on the temperature, the lower the temperature, the better the conditions for the LED and light with higher luminous intensity is generated. To decrease the temperature, it is possible to regulate the current or to use appropriate cooling (heat sinks, fans or both of them are used in headlamps for better air circulation and cooling) [8; 9].

- Advantages

Efficiency: LEDs are the most efficient light sources. They do not need high start energy like xenon bulbs; moreover, they consume less energy when they are in operation [1; 2].

Durability: LEDs do not contain any glass components (like tubes in halogen and xenon bulbs). They are made from solid materials; therefore, they are relatively durable and also shockproof [1; 2].

Flexibility: due to many individual LEDs, any special requirements can be satisfied [1; 2].

- Disadvantages

Price: Purchase price is higher, but in long term LEDs are more economical than halogen or xenon [1; 2].

Cooling: An individual single chip LED does not generate a lot of heat; however, a set made from many LEDs needs to be cooled to avoid damage (heat exchangers of different materials and special printed circuit board (PCB) technologies with or without fans are used to protect LEDs) [1; 2].

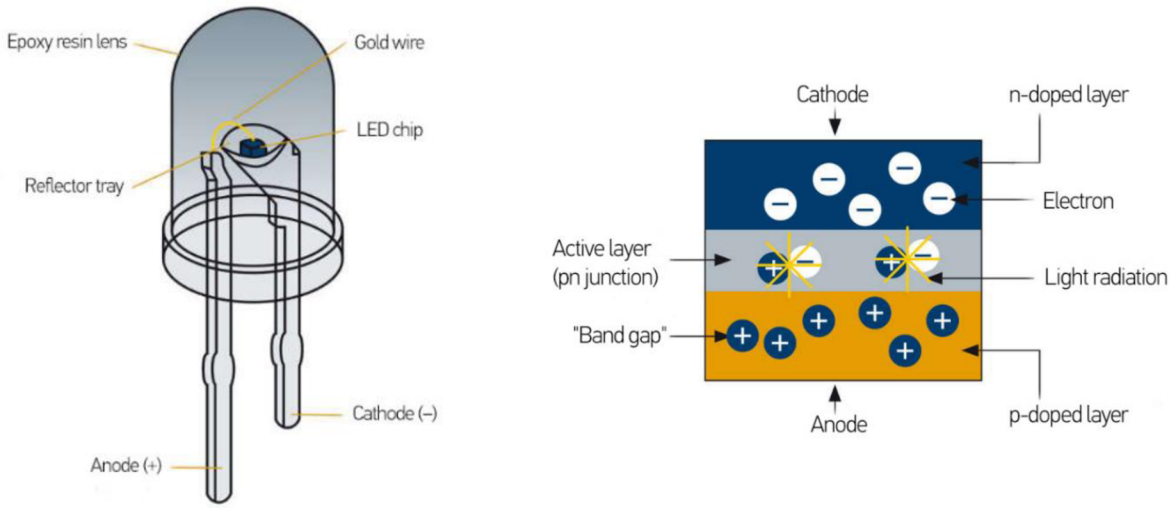

Figure 1.3. Scheme of standard LED with light emitting "PN" active layer [9]

1.4 Comparison light emitters

Table 1.1. Parameters for most expanded light emitters in automotive [1; 3; 8; 10]

Type of lamp	Halogen bulb (H1)	Xenon bulb (DS1)	LED P 3737 (3W)
Light source	Filament	Light arc	LED
Luminous flux	1 550 lm	3 200 lm	366 lm
Capacity	55 W	35 W	3 W
Energy balance	8% Light radiation 92% Heat radiation	28% Light radiation 58% Heat radiation 14% UV radiation	35% Light radiation 65% Heat radiation
Service life (hours)	Approx. 500	Approx. 2 500	25 000 - 50 000
Efficiency	25 lm/W	90 lm/W	127 lm/W
Vibration proof	To a certain extent	Yes	Yes
Ignition Voltage	No	Yes (23 000 V)	No
Electronic control	No	Yes	Yes
Replaceable	Yes	Yes	No
Heat emission	High	High	Low
Cost	Low	Expensive	Expensive
Kelvin temperature (daylight ± 6000 K)	3 200 K	4 500 K	5 700 K
Fuel consumption	0.1 – 0.25 l/100km	0.05 – 0.15 l/100km	0.03 – 0.09 l/100km

In the table 1.1 the most expanded light sources are described. For de-icing issues, energy balance is the most important parameter. Light emitted by halogen and xenon bulbs heats up surroundings; therefore, the ice layer on headlamp de-ices owing to the light source. LEDs are cold light emitters and they do not heat up the illuminated objects. Moreover, the generated heat is discharged from the headlamp by coolers and there is no excess energy for headlamp de-icing, additional process or system must be used for ice removal.

2 THERMODYNAMICS & HEAT TRANSFER

Energy can be transferred by interactions of a system with its surroundings. Interactions could be divided into processes called work and heat. Thermodynamics provides information about the end state process which an interaction occurs, but there is no information regarding to the nature of the interaction or the time rate which it occurs. To determine the behaviour of interaction in time thermodynamic analyses must be extended by the models (physical mechanisms) of heat transfer. Heat transfer is powered by temperature gradients, whenever exists temperature difference between media, heat transfer must occur. There are three types of the heat transfer models, conduction, convection, and radiation [11; 12; 13].

a) b)

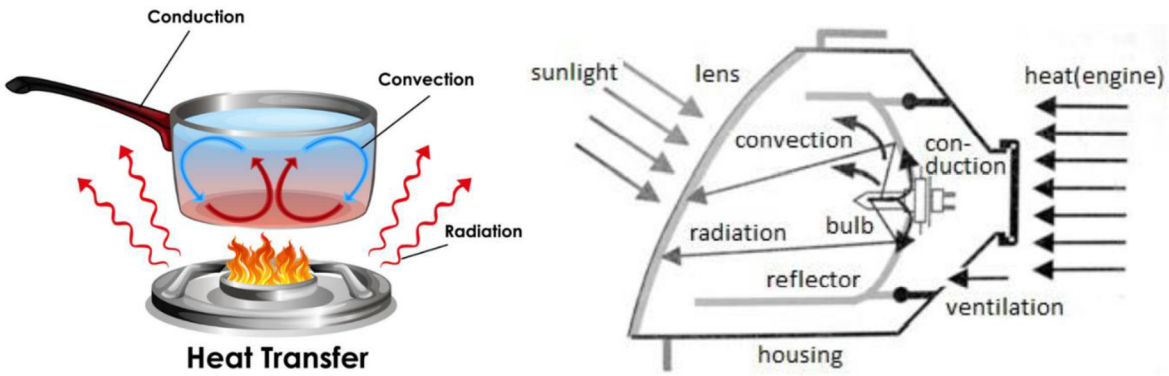

Figure 2.1. Heat transfer in a) daily life [14], b) headlamp [10]

2.1 Conduction

Conduction is the type of heat transfer based on atomic and molecular activity. The energy is transferred from the more energetic particles to the less energetic particles of a substance due to interactions between particles. Higher temperatures are associated with higher molecular energies and during collision energy transfer from more energetic to less energetic molecules must occur. Heat transfer by conduction runs in the direction of a temperature gradient (direction of decreasing temperature) [11; 12; 13].

Conduction applies for all states, for gases and liquids collisions between molecules enhance this energy transfer, for solid materials conduction occurs due to vibrational atomic activity in the form of lattice. For solid materials, which do not transmit radiation, heat transfer by conduction is the only one energy transfer process. In gases and liquids heat transfer by conduction takes place simultaneously with convection and radiation [11; 13].

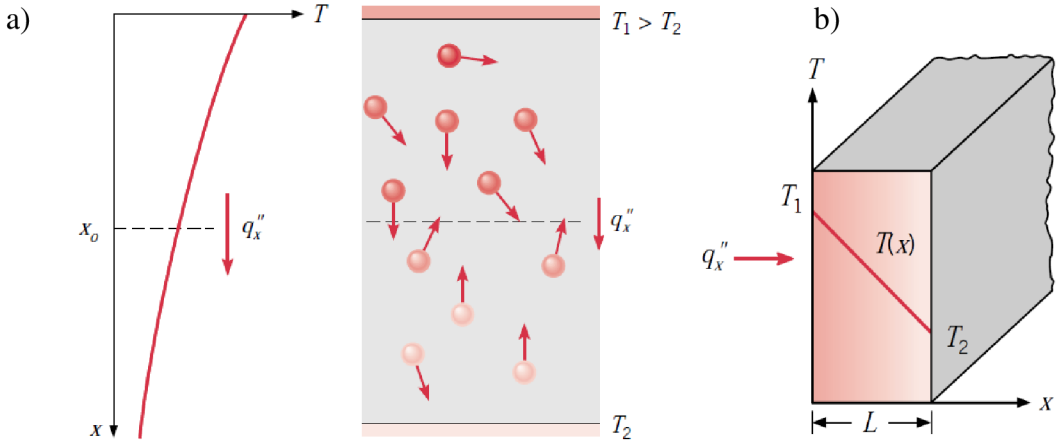

Figure 2.2. a) Conduction by molecular activity, b) one-dimensional conduction [13]

It is possible to quantify heat transfer by conduction in terms of appropriate rate equations. The conduction rate equation is called Fourier's law and it may be used to compute the amount of energy being transferred per unit time [11; 12; 13].

Conductive heat flux: $$q_x'' = -k \frac{\partial T}{\partial x} = -k \frac{T_2 - T_1}{L} = k \frac{\Delta T}{L} \quad (1)$$

- q_x'' is the conductive heat flux [W . m^{-2}]
- k is the thermal conductivity of the body [W . m^{-1} . K^{-1}]
- ΔT is the temperature difference [K]
- L is the thickness of the body [m]

The heat flux q_x'' is the heat transfer rate in the x direction and it is proportional to the temperature gradient $\partial T/\partial x$. Parameter k is thermal conductivity and its value is material property. Heat flux q_x'' represents only the rate of heat transfer per unit area, for calculating heat rate by conduction q_x wall of area A must be specified [11; 12; 13].

Heat rate by conduction: $$q_x = q_x'' . A \quad (2)$$

- q_x is the heat rate by conduction [W]
- A is the wall area [m^2]

2.2 Convection

The convection heat transfer model consists of two mechanisms. First mechanism is energy transfer due to random molecular motion (diffusion), second mechanism is energy transfer by volumetric or macroscopic movement of the fluid. Liquid consists of large number of molecules which moves together or as aggregates. This movement runs in the direction of a temperature gradient and contributes to heat transfer. Because the molecules in the liquid retain their randomness motion, the total heat transfer is calculated as the superposition of energy transfer by random motion of molecules and volume motion of a fluid. Convection is the summary term for both mentioned phenomena [11; 12; 13].

Main representative of convection is heat transfer which occurs between fluid in motion and a bounding surface, both at different temperatures. Result of an interaction between fluid flow and heated surface in the Figure 2.3 is the velocity profile which varies from zero to the finite value u_∞. This area of fluid is known as the hydrodynamic or velocity limit layer. If the temperatures for the surface and flow are different, there will be an area of liquid where temperature varies form T_s at the surface boundary to T_∞ in the outer flow. This area, called the thermal boundary layer and its appearance depends on the flow velocity [11; 13].

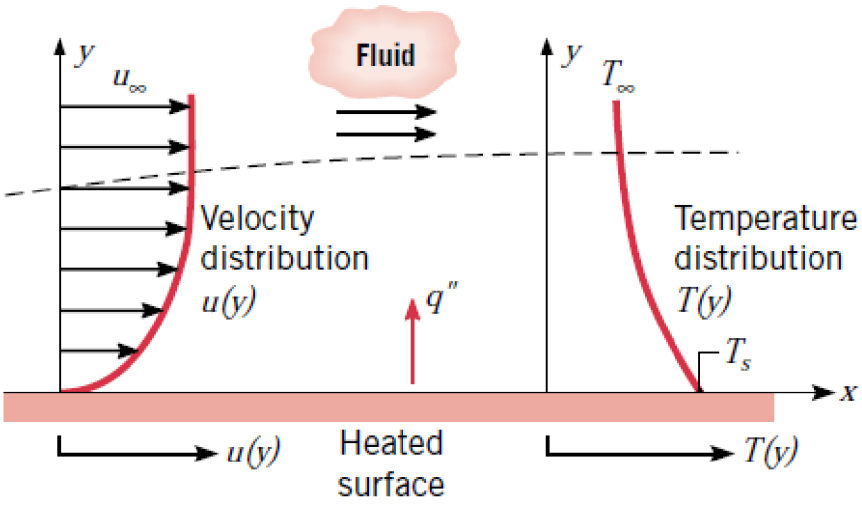

Figure 2.3. Convection heat transfer [13]

Near the surface where the fluid velocity is low convection by random molecular motion (diffusion) dominates. Directly on the surface the flow velocity is equal to zero and energy is transferred only by diffusion mechanism [11; 12; 13].

Convection can be divided into two categories according to nature of the flow. First one is forced convention when the flow is caused by external devices (e.g. fans or pumps), second one is natural convection which is induced by density differences [11; 12; 13].

The appropriate rate equation for convection heat transfer has form: [12]

Convective heat flux: $q'' = h\ (T_s - \ T_\infty)$ (3)

- q'' is the convective heat flux [W . m^{-2}]
- h is the convection heat transfer coefficient [W . m^{-2} . K^{-1}]
- T_s is the surface temperature [K]
- T_∞ is the fluid temperature [K]

The quantity of heat flux is proportional to the temperature difference between surface T_s and fluid T_∞. Parameter h represents convection heat transfer coefficient, which is affected by conditions on the boundary (surface geometry, nature of the flow, etc.). Whole expression is known as the Newton's law of cooling [11; 12; 13].

2.3 Radiation

Thermal radiation is the energy emitted by the matter with non-zero temperature. Emission may occur in all states and it may be attributed to changes in the electron configuration of individual atoms or molecules. The energy of the radiation field is transmitted by electromagnetic waves (alternatively photons), when electromagnetic wave meets any matter, part of the energy is absorbed, the rest is reflected or transmitted. In comparison to the conduction and convection, radiation is independent on the conditions of the surroundings and does not require material medium, the energy is transferred most efficiently in vacuum [11; 12; 13].

Radiation which is emitted by the bounded surface comes from the thermal energy and the rate at which energy is released per unit area (W . m^{-2}) is called the surface emissive power E. The upper limit for the emissive power is described by Stefan-Boltzmann law [13].

Stefan-Boltzmann law (black body): $E_{Black} = \ \sigma\ .{T_s}^4$ (4)

- E_{Black} is surface emissive power [W . m^{-2}]
- σ is Stefan-Boltzmann's constant [5.68 x 10^{-8} W . m^{-2} . K^{-4}]
- T_s is the absolute temperature of the surface [K]

This equation is valid for ideal surface, which is called black body. Black body surface must meet these three conditions: [13; 19]

- It absorbs all incident radiation regardless of wavelength and direction [13; 19].
- Its surface cannot emit more energy than a blackbody for a prescribed temperature and wavelength [13; 19].
- Blackbody is a diffuse emitter (intensity of emitted radiation is independent of direction) [13; 19].

In ordinary world there are practically no objects with black body conditions and the heat flux emitted by real surface is the less than blackbody at the same temperature. Therefore, the black body thermal radiation formula is converted into grey body by emissivity parameter ε [12; 13; 19].

Stefan-Boltzmann law (grey body): $E_{Grey} = \varepsilon . \sigma . {T_s}^4$ (5)

- ε is surface emissivity [-]

Emissivity is the radiative property of the surface. It can take the value from 0 (shiny mirror) to 1 (blackbody), and this value represents how efficiently a surface emits relatively to a black body. The majority of organic, painted, or oxidized surfaces have emissivity values close to 0,95 [11; 13; 19].

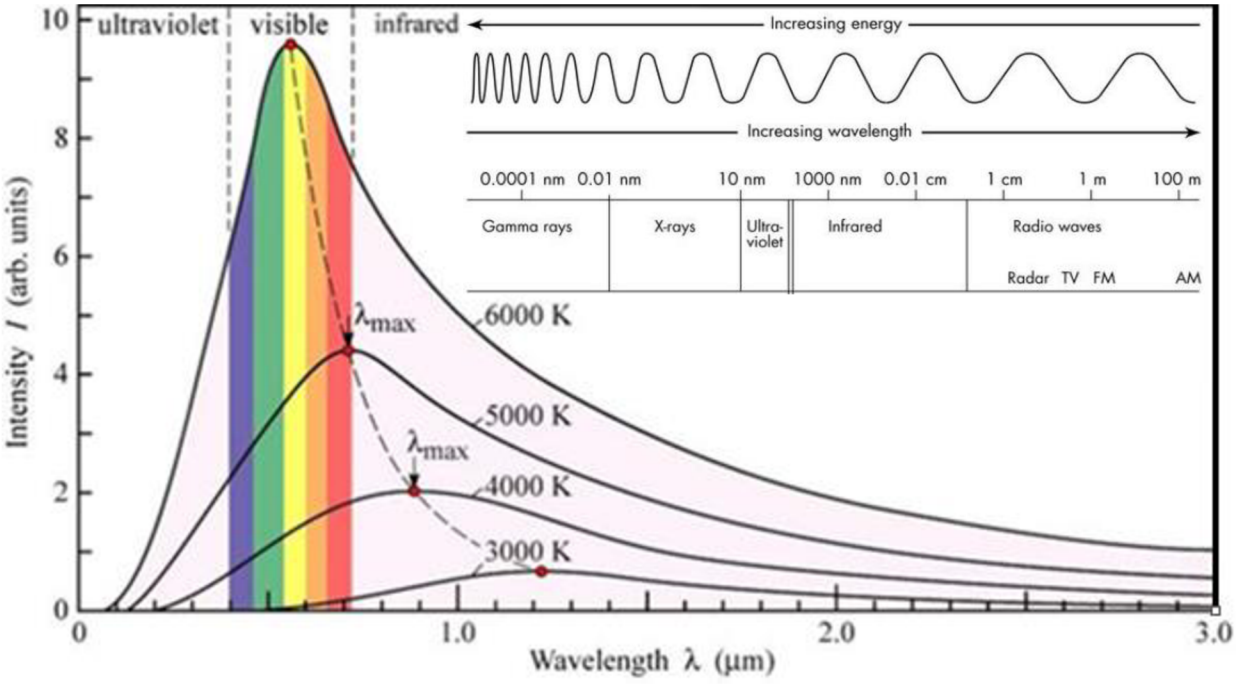

Figure 2.4. Spectral intensity distribution as a function of wavelength for different temperatures [20; 21]

2.3.1 Wien's displacement law

Wien's displacement law should be used for the prediction of the black body spectral distribution. Maximum of the radiated wavelength (wavelength peak) depend on the temperature. Wavelength peaks are inversely proportional to the temperature increase, the higher the temperature, the shorter the wavelength [12; 13; 22].

Wien's displacement law: $\lambda_{Max} = \frac{b}{T}$ (6)

- λ_{Max} is the peak of the radiated wavelengths [m]
- b is Wien's displacement constant [2.897 x 10^{-3} m . K]
- T is the absolute temperature [K]

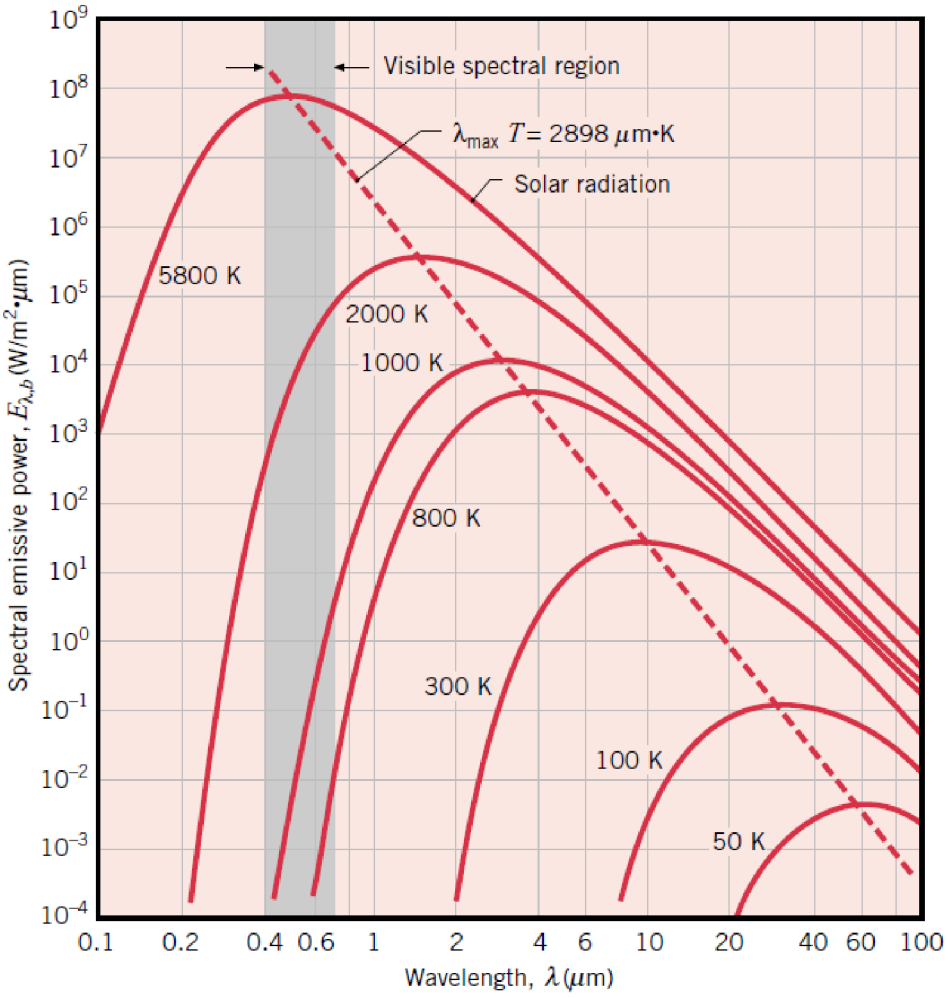

Figure 2.5. Wien's displacement law in the graph [13]

3 SPECIFIC LATENT HEAT

The definition of latent heat is the amount of thermal energy that is absorbed or released by a substance at constant temperature. Typical representatives of constant temperature processes are phase changes (freezing, melting, condensation and vaporization). The thermal energy is called "latent" because it is hidden inside the substance molecules until phase change occurs, "specific" represents expressed energy per unit mass [13; 23; 24].

Latent heat may be imagined as work required to overcome the forces inside the material, which hold the individual atoms or molecules together. Slightly oscillating particles are in the solid regular structure of crystal lattice due to the forces of attraction. As the temperature increases to the melting point, the attraction forces are not able to retain motion of the particles and crystal lattice collapses, material passes from the solid to the liquid phase. In the liquid phase, there are still weak forces of attraction, molecules are free to move but at the same time they have a degree of cohesion. Further temperature increase leads to the boiling point, forces of attraction wear off and liquid passes to gas phase [23; 24].

The specific latent heat depends only on the type of mass, its value is not dependent on the size of the sample or the place where the sample is taken [23].

Latent heat of Fusion: Heat absorbed or released during melting or freezing changes the phase from solid to liquid or vice versa at a constant temperature [23].

Latent heat of Vaporization: Heat absorbed or released during vaporization or condensation changes the phase from liquid to gas or vice versa at a constant temperature [23].

Latent heat formula: $L = \frac{Q}{m}$ (7)

- L is the specific latent heat [kJ . kg^{-1}]
- Q is the heat absorbed or released [J]
- m is the mass of substance [kg]

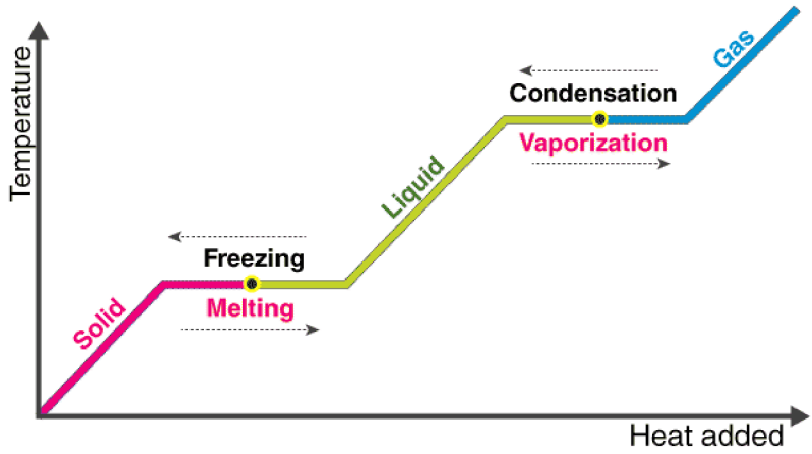

Figure 3.1. Latent heat diagram [25]

4 DE-ICING METHODS

Methods or systems that actively remove an ice layer from the surface. Removal can be mechanical, chemical, or thermal. Mechanical methods are based on the movement and physical force. For chemical de-icing, special fluids are used. The thermal method works on the principle of thermal degradation of ice structure [10; 30].

4.1 Mechanical

- EMEDS

Electro-Mechanical Expulsion De-icing System. Expulsive electromagnetic actuators with elliptical shape are mounted under the skin. When electrical energy is supplied, magnetic field is generated, and elliptical shape is changed to circular. This action causes deflection and gives a force for cracking ice on the skin. Emeds system is shown on the figure 4.1a and it is used exclusively with aircrafts [10].

- Pneumatic de-icing boost

Hollowed rubber strips are fasted on the surface. When the system is activated, air starts to flow inside the rubber strips causing them to expand. The change of the shape breaks the ice layer, then the air is released out and the strips return to the initial shape. The system is also primarily for aircrafts. See figure 4.1.b. [10].

- Wipers

Wipers are intended for cars. They are normally used for removing impurities from the automotive headlamp and they could also be used for ice removing. This system is very effective but without thorough maintenance it is prone to disorders. Wipers are used simultaneously with washer fluid which is sprayed from the nozzles. The system is consisted of many parts, this fact is reflected in the high price; therefore, many manufacturers stopped using the wiper system. Present-day headlamps are made from plastic instead of glass which is also a limitation for wipers that could be scratched; and thus, degrade the headlamp lens. From the mechanical methods, only wipers are usable for car headlamp de-icing (if they do not scratch the headlamp lens), the other systems restrict the passage of light [10].

a) b)

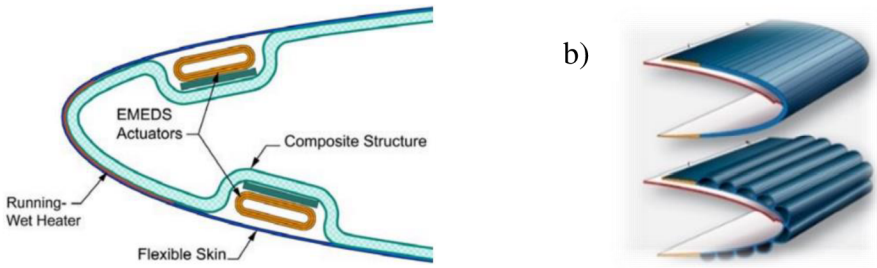

Figure 4.1. a) EMEDS combined with thermal de-icing [26], b) pneumatic de-icing boost [27]

4.2 Chemical

All chemical de-icers work on the same principle, they prevent water molecules from binding under the certain temperature which is under 0 degree Celsius (freezing temperature for pure water). This temperature depends on the concentration of chemical de-icer. For amplification de-icing effect, special chemicals with exothermic dissolution should be used. When exothermic de-icers are in use, thermal energy is generated. This has a consequence in stronger melting power. To the most-commonly known chemicals belong: [10; 28]

- Inorganic salts (sodium chloride, magnesium chloride, calcium chloride) [28].
- Organic compounds (potassium acetate/formate, sodium formate, calcium formate, urea) [28].
- Alcohols, diols, and polyols (methanol, ethylene glycol, propylene glycol, glycerol) [28].

4.3 Thermal

De-icing by using the heat element is directly connected to the aim of this master's thesis; therefore, it will be discussed in more detail. The basic principle of thermal de-icing is temperature increase causing ice to melt away. The drawback of these systems is the time and power efficiency as warming up of the surrounding materials can be a slow process.

4.3.1 Conductive heaters

Conduction is the main type of heat transfer, generally the most direct method of surface de-icing. Conductive heaters are resistive wires or surfaces. They should be glued to the top of the surface or welded into the material. The glued elements are exposed to the environment and there is a risk of wearing off caused by weather or dirt. Therefore, welding is the more durable option. The heating element contains electrodes at the opposite ends which are connected to the voltage source. As the electricity flows through the conductive heater, electric power is converted into thermal energy and heats up the surroundings. The amount of the heat energy is controlled by voltage or current, the higher the quantity, the bigger the amount of heat energy is dissipated. Conductive heaters application directly depends on the material which they are conducted through as the main risk is that the wire becomes too hot and damages the material in contact with [10; 30].

Conductive heaters in automotive are mainly used for back windows. Their application for headlamp lens de-icing is problematic. Special attention must be paid to the heating elements location, inappropriate location affects the passage of light. [10; 29; 30].

4.3.2 Convective heaters

Heat is transferred to the surface by convection, then by conduction through the material. Convective heaters consist of two parts, the heating element (supplies thermal energy to the system) and the circulating device (provides medium circulation in the space). The resistive heaters are mainly used for heat circulated medium; circulator device selection depends on the medium. For air, fans are commonly used, for liquid pumps are used [10; 17; 30].

The process begins in the heater, then the hot air is transported to the required area by a fan. Due to the extra step of heating the air, which is a bad thermal conductor (in many cases, it is used as insulator), convective heaters are not as effective as pure conductive heaters, and the process is slower [10; 30].

The system may be controlled by regulating the fan speed, the heater temperature, or their combination. An option to control system is using Positive Temperature Coefficient (PTC) heaters. The materials with PTC have the ability to increase their electrical resistance when the temperature is raised. The higher the PTC, the greater the increase in electrical resistance for the given temperature increase. Fan regulates only the amount of circulating air [10; 30; 33].

Convective heaters in automotive are mainly used for windshield de-icing or defogging. Application in headlamps is also possible as the hot air does not affect the passage of light. The system can be placed anywhere in the headlamp if there is an open way for air circulation to the required area. It is necessary to take the position into account as the effectivity declines non-linearly with the distance of the object. Further disadvantage of the convective heaters is that the complicated fans consist of many parts with susceptibility to vibration damage [10; 30].

4.3.3 Radiant heaters

Radiant heaters mainly warm up the surroundings by radiation in Infra-Red (IR) spectrum, whereas the radiation spreads from the heat element to the surroundings by waves. The radiated wavelength corresponds with the heat element temperature (see Temperature & Heat Transfer: Radiation). Therefore, it is necessary to keep the constant temperature to obtain optimal wavelengths in IR spectrum. Optimal wavelengths are dependent on the absorbing material. For every material, there is a different absorption curve. If radiated wavelengths correspond with material absorption peaks, efficiency is on the maximum. The energy dissipated through the air between the radiant heater and the receiver can be often neglected. The influence of radiated IR waves on the headlamp functionality or light distribution is negligible and the heaters could be placed where the passage of light is not affected by them. Therefore, the radiant heaters could be successfully implemented into car headlamps [10; 30; 31].

Radiant heaters should be controlled by the same manner as conductive heaters. They convert electric energy into thermal energy owing to the resistive elements. The amount of the delivered electric energy corresponds with the heat element temperature, and the radiated wavelengths are dependent on the temperature [10; 30].

Nowadays for automobile headlamp production plastic materials are mainly used. Typical material for cover lens production is called Makrolon polycarbonate. It looks like glass or plexiglass, but in contrast to these materials is practically unbreakable (impact resistant due to high material toughness). Makrolon has got also good workability and high wavelength transmission in visible part of spectrum.

Icing formed on the outer side of the Makrolon headlamp cover lens can be removed by radiant heaters, but it is necessary to found IR element with relevant parameters. Efficiency of de-icing process directly depends on the energy transfer between IR element and cover lens. Optimal IR element radiates wavelengths in absorption peaks (regions with the lowest transmission) of Makrolon polycarbonate. The first absorption peak of Makrolon is around 1650 nm (see figure 4.2.), from Wien´s law (see Temperature & Heat Transfer: Wien's displacement law) the absolute temperature 1756 K (1483 °C) can be calculated for wave radiation in this part of IR spectrum. This temperature is achievable on the IR element; however, there is a problem with headlamp components as the majority of the parts is made from plastic with low temperature endurance. Application of hot IR element in the headlamp requires appropriate precaution, for example active protection (control systems evaluating conditions in the headlamp) or strong fixation concept. This combination increases the weight and price of the headlamp [30].

A possible solution of this problem (high temperature on the IR element) is using longer wavelength absorption peaks. Makrolon has got high absorption in longer wavelength spectrum and lower temperatures are required on the IR element. The amount of transferred energy is lower but there is also a lower risk of damaging the plastic parts around the radiant heat element.

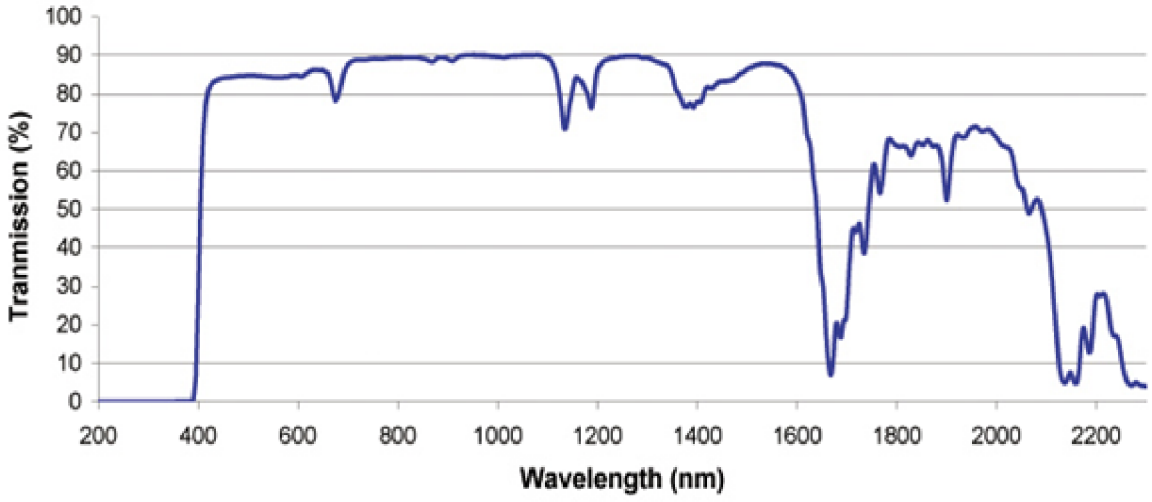

Figure 4.2. Makrolon polycarbonate sheet spectral transmission [32]

4.4 Summary of the de-icing methods

Table 4.1. Summary of the de-icing methods

De-icing system	Advantages	Disadvantages
Mechanical wipers	High effectivity, quick ice removing	Mechanically complicated system prone to disorders. Wipers could scratch and damage the headlamp lens made from plastic materials (plastic is not as durable as glass lenses used in the past)
Chemical	Faster de-icing than thermal methods	Used chemicals might be expensive and non-environmentally friendly. Other requirement is to observe the amount of liquid and top it up when necessary
Thermal conductive heaters	Most efficient way of surface de-icing (resistive wires or surfaces are in close contact with the ice layer), also these systems are very durable against the shocks caused by vibration	Inappropriately placed heat elements (resistive wires or surfaces) restrict the passage of the emitted light and devaluate headlamp
Thermal convective heaters	The system may be placed anywhere in the headlamp (does not restrict passage of light), but longer distance impacts the efficiency (non-linearly decrease)	Complicated systems composed from many moving parts, which are prone to damage caused by vibration shocks. Efficiency is lower than for the conductive heaters due to the extra step in heat transfer (heat is transferred by air which is a bad conductor)
Thermal radiant heaters	If the wavelengths are emitted in absorption peaks of the receiving material, energy transfer achieves high efficiency. IR element should be placed outside of the passage of light	Risk of overheating the surrounding elements due to the high IR element temperatures

In present-day world, the radiant heat elements are used in truck headlamps as a de-icing system and the lens is made of Makrolon. In demanding climatic conditions, headlamp icing is a common issue, and a numeric simulation model is needed for the prediction and a subsequent optimization of the de-icing behaviour (the determination of the time required for the vehicle's operability).

5 SIMCENTER STAR-CCM+

Simcenter STAR-CCM+ is a Computational Aided Engineering (CAE) system for solving fluid and solid mechanics problems. It offers many options for engineering analyses, such as import and creation of geometries, mesh generation, solution of the governing equations, analysis of the results and many others. For easier orientation object tree is used in simulation, main points will be discussed in this chapter [15].

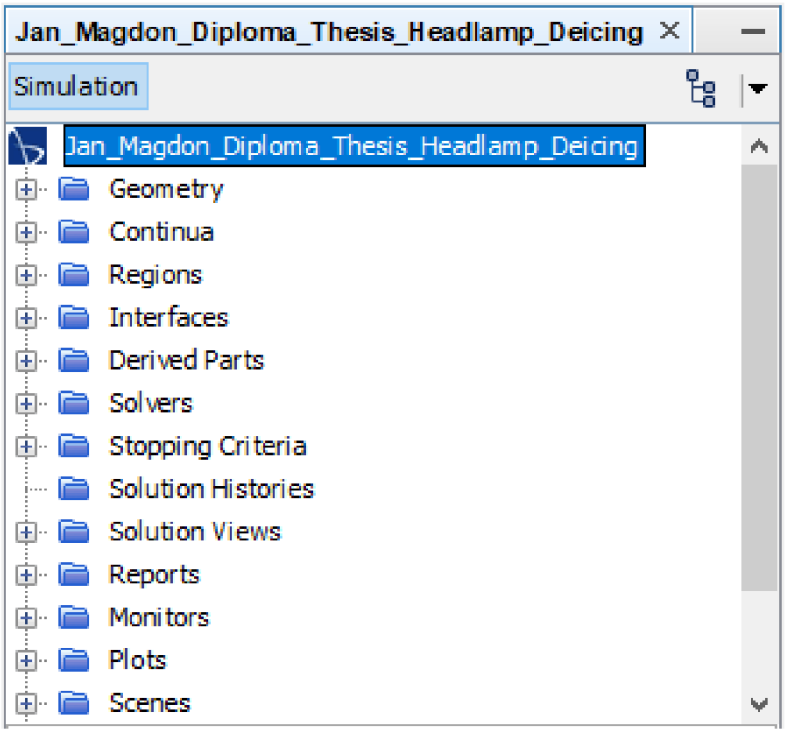

Figure 5.1. Simulation object tree in Simcenter Star CCM+

5.1 Geometry

For geometry import Simcenter Star-CCM+ reads data in native formats (Catia V5, Siemens NX, Inventor), neutral formats (IGES, STEP), triangulated formats (STL) and PLM formats. It is used for geometry modification and creation of parametric feature-based modeler, which is supported on Windows or Linux [15; 16].

5.2 Continua

Continua are used to store information about physics or meshing models that are subsequently applied to one or more regions, currently continua are not geometrically associated with them [15].

a) Mesh continuum

Contains a selection of meshing models, operations are divided into surface and volume meshing. Surface meshing provides high quality triangulations and tools for surface preparation (repairs and prepares surfaces), wrapping (provides closed surfaces) and remesher (provides high quality surfaces for volume mesh). Mesh topologies for surfaces are triangles, quadrilaterals, and polygons. Volume meshing allows automatic volume mesh generation with optimized cell quality, it includes core general meshers (trimmed, polyhedral or tetrahedral) or specialized meshers for particular geometry (thin or extruder mesher) [15; 16].

b) Physics continuum

Physics setting is provided by models including fluid and solid mechanics, heat transfer, electromagnetism, and chemical reactions. In the macroscopic scale (the lengths are much larger than the atomic distances), structure of the matter may be neglected, and the material may be modelled as continua. Star-CCM+ solves system of equations derived from the fundamental laws of physics which express conservation principles (Eulerian or Lagrangian approach). Each physics continuum represents the single substance which occurs in the applied regions [15; 16].

In Star-CCM+ these models are available: [15; 16]

- For modelling of fluid flow and energy in fluid mechanics the flow characteristics are used (laminar, turbulent, viscosity, compressibility, multiphase mixtures), temporal discretization (steady or unsteady) and equation state (ideal or real gas law, density).
- For common materials in categories of solid, liquid, gas and electrochemical types, there is a database, or user defined materials should be used.
- Heat transfer in solid and fluid materials is simulated by conduction, convection and radiation (surface to surface model, solar loads etc.)
- Turbulence is solved by Reynolds averaged Navier Stokes models (K-Epsilon or K-Omega), Reynolds stress transport models or laminar-turbulent transition (Gamma ReTheta model).
- Multiphase flow is divided into **Eulerian** and **Lagrangian** description.

Eulerian models observe the particles, bubbles or droplets to be a continuum passing through a fixed volume. This category includes Eulerian Multiphase Segregated Flow (EMP), Volume of Fluid (VOF), Fluid Film (FF), Dispersed Multiphase (DMP) and Mixture Multiphase (MMP) [15; 18].

Lagrangian models tracks parcels of particles as they move through space and time. Representatives are Lagrangian Multiphase and Discrete Element Method (DEM) [15; 18].

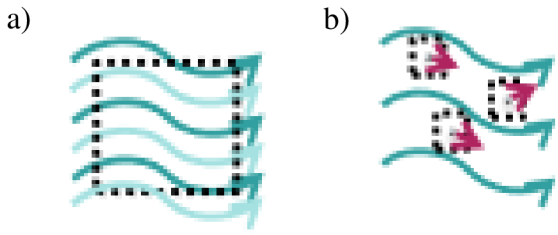

Figure 5.2. a) Eulerian model, b) Lagrange model [18]

Star CCM+ can solve many other problems, for example reacting flows, electrochemistry, plasma, electromagnetism, and aeronautics. However, these topics are not the main focus of this master's thesis [18].

5.3 CAD model division

The input for the simulations are 3D CAD models, which are served as background for the simulation experiments. However, the 3D CAD model without additional parameters is not enough for the simulation, it is necessary to determine the properties of individual parts in order to be applicable to numerical models. CAD model division for simulation application is shown below in this chapter.

- Regions

Regions are volume or planar domains in space, limited by boundaries. Boundaries are not shared between the regions. Information transfer is provided by interfaces, which connect one region to another [15; 16].

The type of the region depends on the material model selected in continua. In Simcenter Star-CCM+ there are three main types of regions, fluid (gas or liquid continuum), solid (solid continuum) and porous (gas or liquid continuum in combination with porous media modelling) [15; 16].

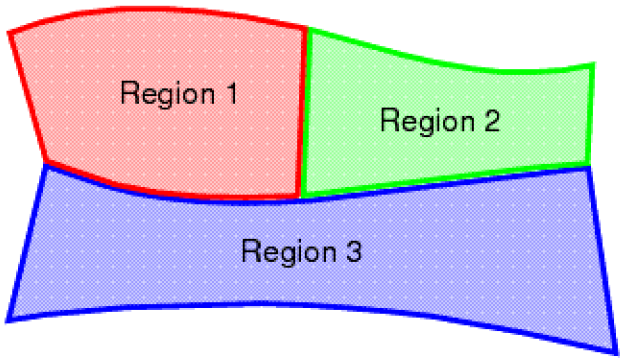

Figure 5.3. Regions [15]

- Boundaries

Boundaries are surfaces (for volume regions) or lines (for planar regions) which surround and define regions. Boundary can be found in the object tree under region section, each boundary has its own properties and setting. Boundary is not shared between the regions. It belongs to only one region [15; 16].

The type of the boundary indicates behaviour of the region during simulation. Boundary could be set as velocity, pressure or mass inlet/outlet which affects the motion of fluid regions. Fixed, free, pressure or force solid stress boundaries are used for defining solid regions. If there is no action on the boundary, the boundary is set as the wall [15; 16].

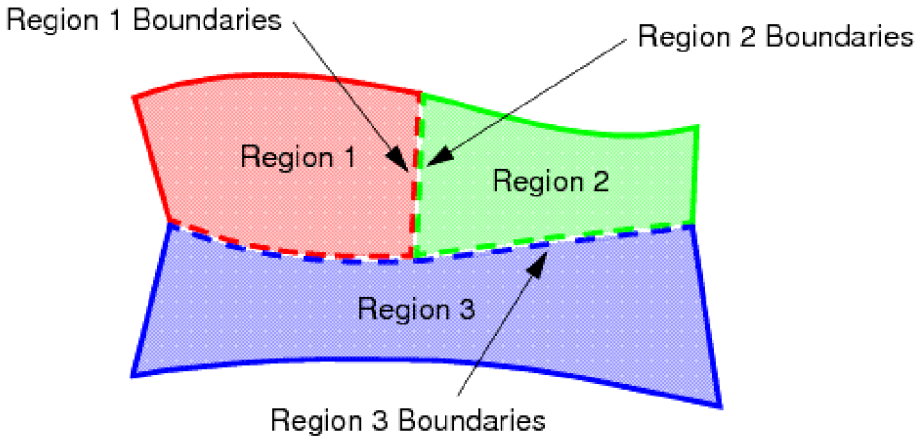

Figure 5.4. Boundaries [15]

- Interfaces

Interfaces provide the connection between regions. They are consisting of two coincident boundaries between two regions and permit mass, energy or other continuum quantities pass from one region to another [15; 16].

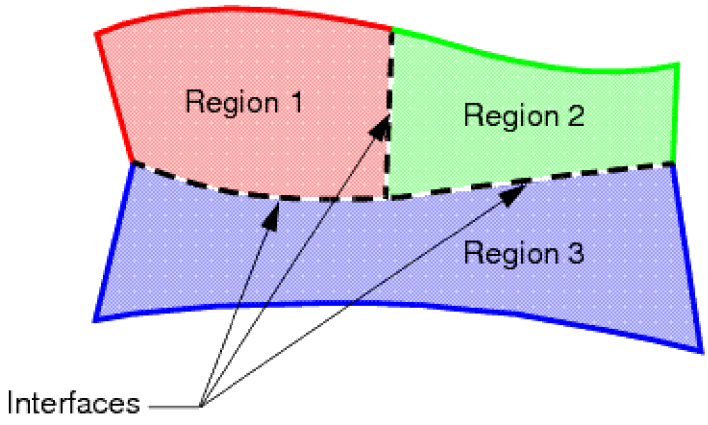

Figure 5.5. Interfaces [15]

5.4 Solvers

Solvers are numerical algorithms which solve the system of matrix equations in finite element method (FEM) or finite volume method (FVM). They are created from the physics models and their boundary conditions [15].

- Finite Element Method (FEM)

CAD model is divided into finite element mesh, which is represented by small but finite elements of geometrically simple shapes. The next step is defining the required physics for each element in the mesh, mathematically described by partial differential equations. These equations are solved by approximating the fields in each element as a simple function (linear or quadratic polynomial), which provides a rough description of the local physics. By connecting all the elements, a large system of sparse matrix equations is obtained, which can be solved by any known sparse matrix solvers. The type of solver used depends on the original physics and gives a unique imprint on the structure of the matrix [34; 35].

- Finite Volume Method (FVM)

In the beginning, finite volume method is similar to the finite element method, CAD model is divided into very small but finite elements of geometrically simple shapes. After that, these two methods differ considerably as a mesh composed of simple geometric shapes is transformed into volume cells which create volume mesh [34; 35].

The finite volume method is based on the fact that many physical laws are a law of conservation - what goes into one cell on the one hand must leave the same cell on the other. The finite volume method is therefore based on flux conservation equations defined as an average value of the cells. Today, this method is very successful in solving fluid flow problems [34; 35].

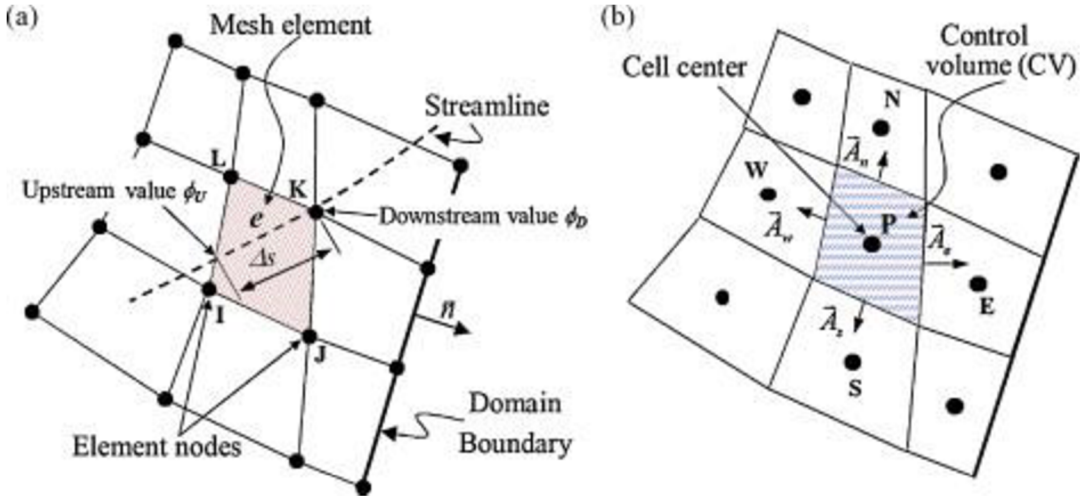

Properties are calculated for every node based Uses Taylor series	Properties are calculated for every cell instead of node based Uses Divergence theorem

a)

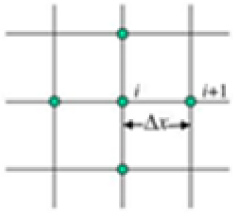

b)

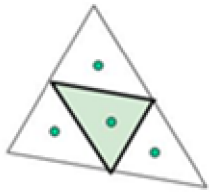

Figure 5.6. Differences between a) FEM, b) FVM [36; 37]

There are two options how to store data from numerical algorithms (solvers), precision represents the size of floating-point data.

- Single precision

  Occupies 4 bytes of memory, this value represents 7 digits of precision [18].

- Double Precision

Occupies 8 bytes of memory and has 15 digits of precision. This option is used for cases when physical phenomena is in vastly different scales, for example microstructure battery modelling, electrodynamics simulations and multiphase flows [18].

The advantage of double precision simulations is increased accuracy and then less round-off errors, this results in robust converge solution [15; 18].

The disadvantages are of course memory requirements, which are 20% higher than in single precision version. The size of the simulation is increased by not more than 100% and overall simulation time is increased by 15-20% [15; 18].

5.5 Stopping criteria

Stopping criteria specify limitations for simulation, they restrict how long simulation runs and under what conditions simulation stops iterating. Each entered criterion is evaluated after the calculation of each step of the simulation and a logical rule is used to determine whether the interaction of all criteria will stop the solver. In Simcenter Star-CCM+, the stopping criteria should be generated automatically (criteria are generated automatically when a solver is chosen) or manually (especially criteria connected to existing monitors which provided more meaningful criteria to judge convergence) [15].

5.6 Data analysis

Simcenter Star-CCM+ provides the tools for analysing simulation result numerically and visually.

- Reports

There are 3 types of reports, system reports (information about performance and memory), statistical reports (apply statistical functions to data within the simulation) and specific reports (information relevant to specific physical models) [15; 16].

- Monitors

Monitors are used for sampling and saving information from the simulation during the solution. Monitors should be report-based (recording changing report values as the simulation progressed) or field-based (collect data from all or a part of solution domain; the types are maximum, minimum, sum, variance etc.) [15; 16].

- Plots

Plots are graphical data displays, for Simcenter Star-CCM+ they are fully customizable. The plots are divided into monitor plots (displays collect report-based monitor values as the solution proceeds), XY plots (two-dimensional graphs that are able to display scalar values form the table data) and histogram plots (two-dimensional bar charts for displaying data severance) [15; 16].

- Scenes

Visualization is provided by graphical scenes and accessory displayers. Specific appearance depends on the type of a displayer, scenes are fully customizable. For simulation, any number of the scenes with any number of the displayers are available. Simcenter Star CCM+ offers default scenes (geometry, mesh, scalar, vector or empty), representation could be changed in global scene controls (lighting, transparency, annotations) and there are also post-processing entities (scalar field display, 2D and 3D vector glyphs, streamlines, section slices etc.) [15; 16].

5.7 Usability & Productivity

Simulations could run as local jobs or remote jobs on a cluster. For work facilitation, all functions could be automated using Java macros. Java macros should be recorded, edited and written in Simcenter Star CCM+ by the client, or they should be written and compiled as a user code that is executed by the server [15].

PRACTICAL PART

6 INTRODUCTION TO RESEARCH

The reason for the elaboration of this master's thesis is an improvement in the field of headlamp light sources. Today LED light sources are widely used and as already mentioned in previous chapters, the heat generated by the LED is dissipated from the headlamp by the heat sinks and coolers, and these light sources contribute to the temperature increase inside the headlamp less in comparison to halogen or xenon light sources. In demanding climatic conditions, a layer of ice may form on the headlamp cover lens. Ice layer restrict the passage of the light and causes inoperability of the vehicle. Especially for the large truck headlamps is difficult to remove ice layer, because there is not enough power for temperature increase inside the headlamp (large volume of air needs a lot of energy to heat up) and melting ice away. The de-icing process will take a long time or will not take place at all.

This Master's thesis gives an insight into research in de-icing simulations. Simulations can predict de-icing behaviour and thus they can help with development and design optimization of the headlamp. Simulations can also answer the question, how long it will take for a car to be operable. This factor can be one of the customer's requirements and therefore it is an important information.

Figure 6.1. Ice layer on the headlamp cover lens [38]

7 SIMULATION MODEL DESCRIPTION

For purpose of an efficient calculation of a large number of simulations in a short time, a simple model might be used. Simple means a small model with no difficult geometry, which could be meshed easily. Size of the model is directly connected with computation time. In addition, it is also easier to work with smaller amount of data.

7.1 Individual parts of the simulation model

Simulation model in this master's thesis consists of continua and regions below. The definition of continua and regions is provided in the following subsections.

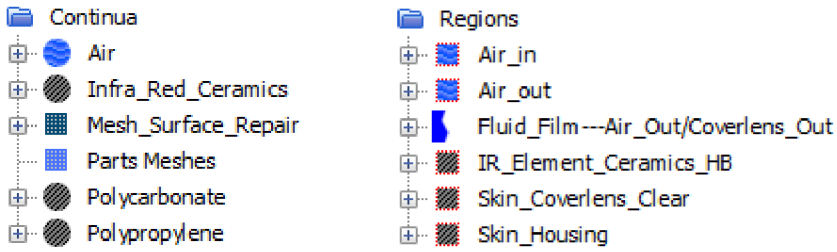

Figure 7.1. Continua and regions from the simulation tree

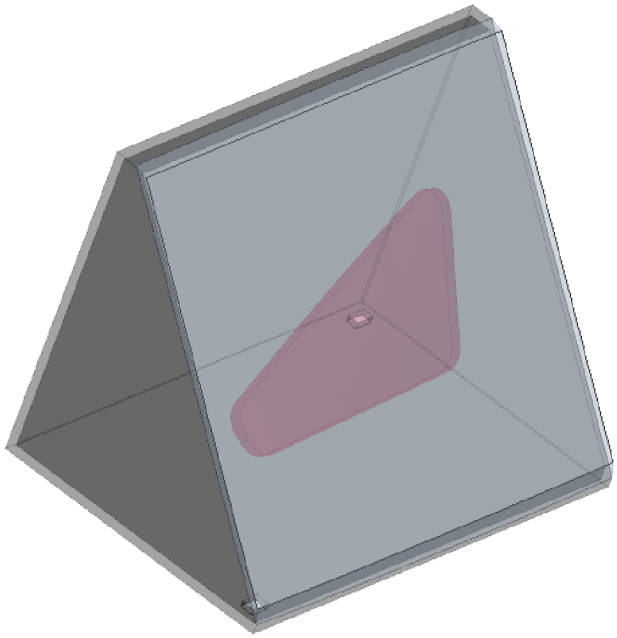

Figure 7.2. De-icing CAD model used for the simulations

7.1.1 Continua

On a macroscopic scale, every material has cracks and various deformations, but some properties affect the whole material as a continuum. This is the basic concept of continuum mechanics. These properties are modelled on the assumption that the mass fills the entire area of space, without cracks, deformations, different molecular structures, atoms, electrons, or distributed densities, but it is a single entity with a one set of parameters [18].

Table 7.1. Used values for the individual continua [39; 40]

Liquid	Air	Reference values	Gravity [m . s^{-2}]	[0; 0; 9.81]
			Reference Altitude [m]	[0; 0; 0]
			Min Allowable Wall Distance [m]	1.0e-6
			Max Allowable Pressure [Pa]	1.0e8
			Min Allowable Temperature [K]	100,0
			Min Allowable Pressure [Pa]	1000.0
			Max Allowable Temperature [K]	1800.0
			Reference Pressure [Pa]	101325.0
		Initial conditions	Pressure [Pa]	101325.0
			Static Temperature [K]	272.65
			Turbulence Intensity [-]	0.01
			Turbulent Velocity Scale [m . s^{-1}]	1.0
			Turbulent Viscosity Ratio [-]	10.0
			Velocity [m . s^{-1}]	[0; 0; 0]
		Material Properties	Density [kg . m^{-3}]	1.18415
			Dynamic Viscosity [Pa . s]	1.85e-5
			Specific Heat [J . kg^{-1} . K^{-1}]	1003.62
			Thermal Conductivity [W . m^{-1}. K^{-1}]	0.02603
			Turbulent Prandtl Number [-]	0.85

Solid	IR_Ceramics	Reference values	Min Allowable Temperature [K]	100.0
			Max Allowable Temperature [K]	1800.0
		Initial conditions	Static Temperature [K]	272.65
		Material Properties	Density [kg . m^{-3}]	3000.0
			Specific Heat [J . kg^{-1} . K^{-1}]	850.0
			Thermal Conductivity [W . m^{-1} . K^{-1}]	2.6

Solid	Polycarbonate	Reference values	Min Allowable Temperature [K]	243.15
			Max Allowable Temperature [K]	394.15
		Initial conditions	Static Temperature [K]	272.65

		Material Properties	Density [kg . m^{-3}]	1200.0
			Specific Heat [J . kg^{-1}. K^{-1}]	1100.0
			Thermal Conductivity [W . m^{-1}. K^{-1}]	0.19
Solid	Polypropylene	Reference values	Min Allowable Temperature [K]	263.15
			Max Allowable Temperature [K]	430.15
		Initial conditions	Static Temperature [K]	272.65
		Material Properties	Density [kg . m^{-3}]	920.0
			Specific Heat [J . kg^{-1}. K^{-1}]	1900.0
			Thermal Conductivity [W . m^{-1}. K^{-1}]	0.14

7.1.2 Regions

Regions are assigned to a certain continuum and assume their properties unless specified otherwise. Regions are domains of volumes representing geometries under consideration (applies for 3D) in space and they are completely surrounded by boundaries. Each region has a unique name, and it can be renamed according to the convenience of the user.

- Air

Air is in surrounding of all the parts, inside the housing (Air_In) and outside the housing (Air_Out). In the system there are no additional devices to affect the air flow or energy transfer, all changes are caused only by the temperature increase in the heat source (IR element).

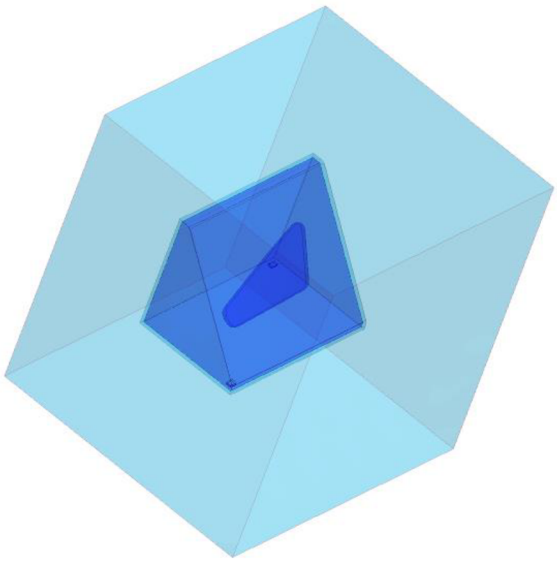

Figure 7.3. Air_In (dark blue) and Air_Out (light blue) region

- IR Element

IR element was used as an energy source for the de-icing process. The temperature of the IR element can reach high values, so it is necessary to use material with high temperature endurance. One of many suitable materials is a ceramic, which meets requirement of high temperature endurance and in addition it is not subject to oxidation, also can be modelled into various shapes. Instead of Joule heating model, total heat energy source was used as physics condition due to the simplicity. Time required for the de-icing process works on the presumption that the higher the energy dissipates, the faster the de-icing process is, due to this fact higher values (power in watt) have been used for the total heat source.

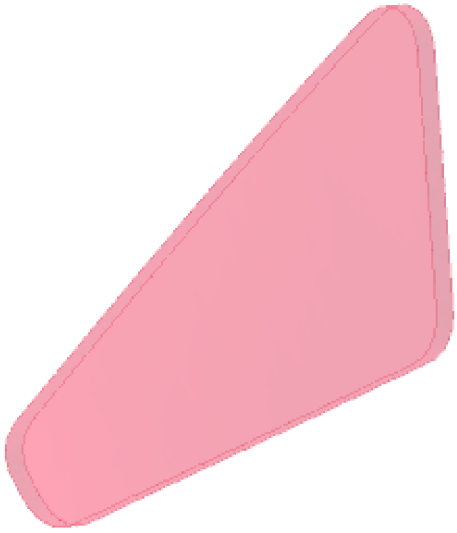

Figure 7.4. IR element region

- Housing

Housing is considered to be from polypropylene, same material is used for the car headlamp housings. Polypropylene has very good chemical and mechanical resistance, other key characteristics include unyielding, strength (despite its low weight), acceptable resistance to heat and low flammability. Due to its composition, polypropylene is not susceptible to internal tension and it is resistant to UV radiation and the effect of solvents.

Heat transfer takes place through the polypropylene housing via the heat conduction, also inside the housing is Air_In, which is connected to the Air_Out around housing by holes in the wall, so the flow and energy exchange can take place between these regions. Housing also contains an IR element that is placed parallel to cover lens.

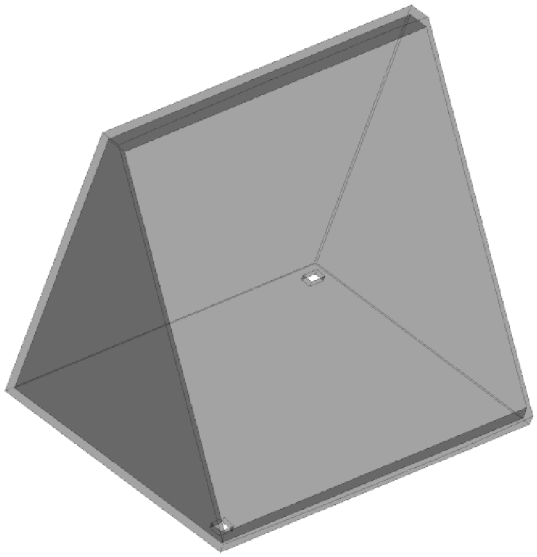

Figure 7.5. Housing region

- Cover lens

Cover lens is made from Makrolon polycarbonate (material typically used in car headlamps), which is extremely robust, lightweight with glass-like transparency and it is impact resistant, even at low temperatures [41].

In the simulation, ice layer is modelled on the cover lens. Ice film model is the shell region with a zero thickness and is created between outer boundary of the cover lens and Air_Out boundary.

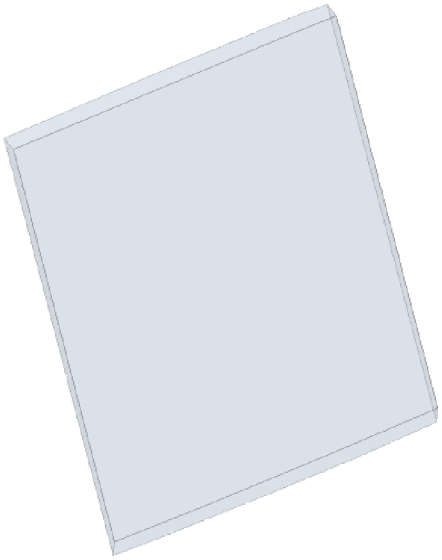

Figure 7.6. Cover lens region

7.1.3 Mesh

For meshing operations polyhedral, thin and prism layer meshers were used. For surface mesh operations surface remesher and automatic surface repair were used. Other parameters for the mesh generating are in the table 7.2.

Table 7.2. Used meshing parameters for the individual regions

Liquid	Air_In	Custom values	Target Surface Size [m]	1.0e-3
			Minimum Surface Size [m]	5.0e-4
			Prism layers [-]	3
Liquid	Air_Out	Custom values	Target Surface Size [m]	5.0e-2
			Minimum Surface Size [m]	2.5e-2
			Prism layers [-]	3
Solid	IR_Ceramics	Custom values	Target Surface Size [m]	2.0e-3
			Minimum Surface Size [m]	1.0e-3
			Prism layers [-]	3
Solid	Housing	Custom values	Target Surface Size [m]	3.0e-3
			Minimum Surface Size [m]	1.5e-3
			Prism layers [-]	3
Solid	Cover lens	Custom values	Target Surface Size [m]	3.0e-3
			Minimum Surface Size [m]	1.5e-3
			Prism layers [-]	3

Between solid and fluid regions prism layers were activated. Prism layers are formed by prismatic cells next to wall surface boundaries. The main advantage of prismatic cells is higher accuracy of the flow solution. Especially for the turbulence flow modelling, 10 – 20 cells in the cross-steam direction are required for an accurate resolution. This amount should be replaced by a few prism layers [18].

The mesh quality is directly connected to the computational time and data size of the simulation, so it is necessary to set optimal parameters. With a fine mesh, more accurate results can be expected at the expense of computational time (it takes more time to solve equations for more cells). In the simulation it is necessary to identify regions where major changes are expected. For these regions fine mesh parameters must be set otherwise the simulation can become inaccurate. The size of a cells also affects the stability of the simulation. If significant physical changes occur in a region with cells which are large in size, the solver may not be able to solve equations over the cell or the solution becomes inaccurate (see chapter 8.1 Simulation stability: Courant number).

In solid regions, where heat transfer by conduction is the main type of heat transfer and the occurrence of significant physical changes is low, relatively rough mesh was used. In liquid regions situation is different, in Air_Out large cells were used because this region is not subject to observation and accurate results are not required. In comparison to Air_In small cells were used, because this region serves as medium for energy transfer between IR element and ice layer on the cover lens. Temperature changes in this area are noticeable, convection is the main type of heat transfer here and causes high energy flow in this region.

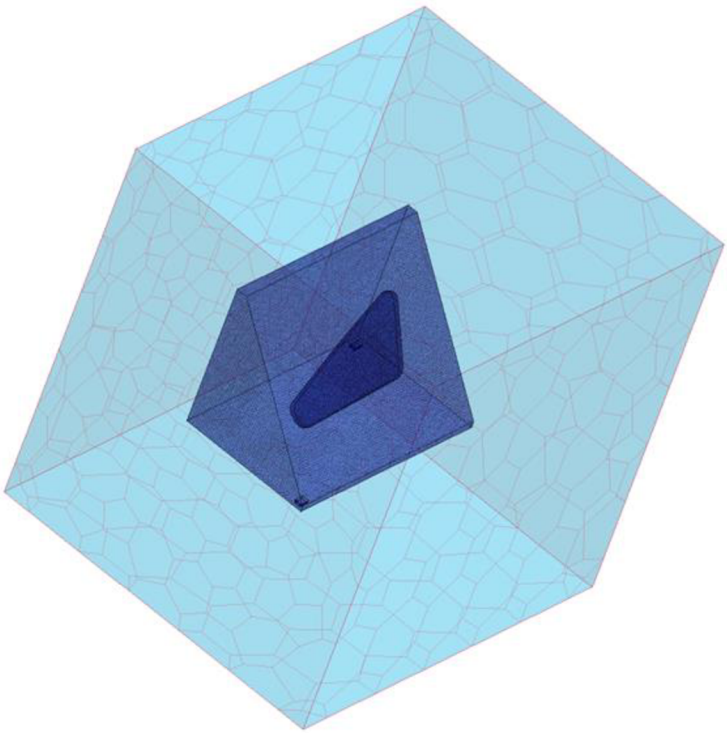

Figure 7.7. Mesh comparison for regions Air_In (dark blue) and Air_Out (light blue)

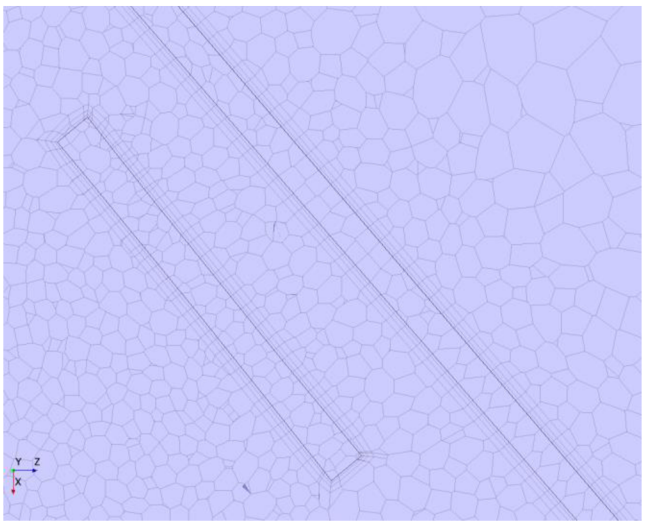

Figure 7.8. Prism layers in the cut view through the Air_In, IR element and cover lens regions

7.1.4 Models

- Models suitable for de-icing:

For de-icing application, a few models can be used in Simcenter Star CCM+. Main representatives are models Fluid Film (FF), Thin Film (TF) and Volume of Fluid (VOF). Each of these models has got its advantages and disadvantages, which are shown below:

a) Thin Film

Thin film is the model which can provide an insight into de-icing and de-fogging processes. It is suitable for simulations where the thin film thickness is negligible compared to the cell size, thus to this fact it is used primarily for de-fogging processes.

Application of the thin film model for the de-icing has got one big disadvantage. Ice layer melting may occur although there is not enough energy for phase change, i.e., melting can easily occur below freezing point of the water. This solution cannot be taken as credible, and it is why this model cannot be used for any realistic de-icing simulations and will not be considered in this master's thesis. [18].

b) Volume of Fluid

Volume of fluid is a multiphase model treating ice layer as 3D part, which is designed in the simulation geometry. Due to non-zero thickness of ice layer in VOF model it is more suitable for thick ice layer regions where thickness plays a significant role.

The biggest disadvantage of the VOF model is the ice layer definition, it is not possible to change ice layer thickness easily by one parameter. Individual geometrical part must be adapted or replaced by a new one and simulation must be remeshed. For small sized simulations it would not matter so much, but for the whole headlamp simulation with millions of cells it can take long time. Try-out simulations applying this model were performed but the model was not the main focus of the thesis.

c) Fluid Film

For the purposes of this master's thesis fluid film model was chosen. This model is based on the shell region, which is not modelled as a part in geometry, but it is modelled as shell region between two boundaries. This shell region has physically zero thickness, as thickness is set only in the fluid film model in initial conditions (see chapter 7.1.5: Focus on the fluid film model).

The main advantage of fluid film model is the ice thickness variability, which can be easily modified in initial conditions without remeshing simulation model. The main disadvantage is physical zero thickness of the shell, which results in the instability of the simulation for higher ice thicknesses. For these cases short time steps must be used, otherwise the simulation can become unstable [18].

In figure 7.9. individual models used in the simulation are shown.

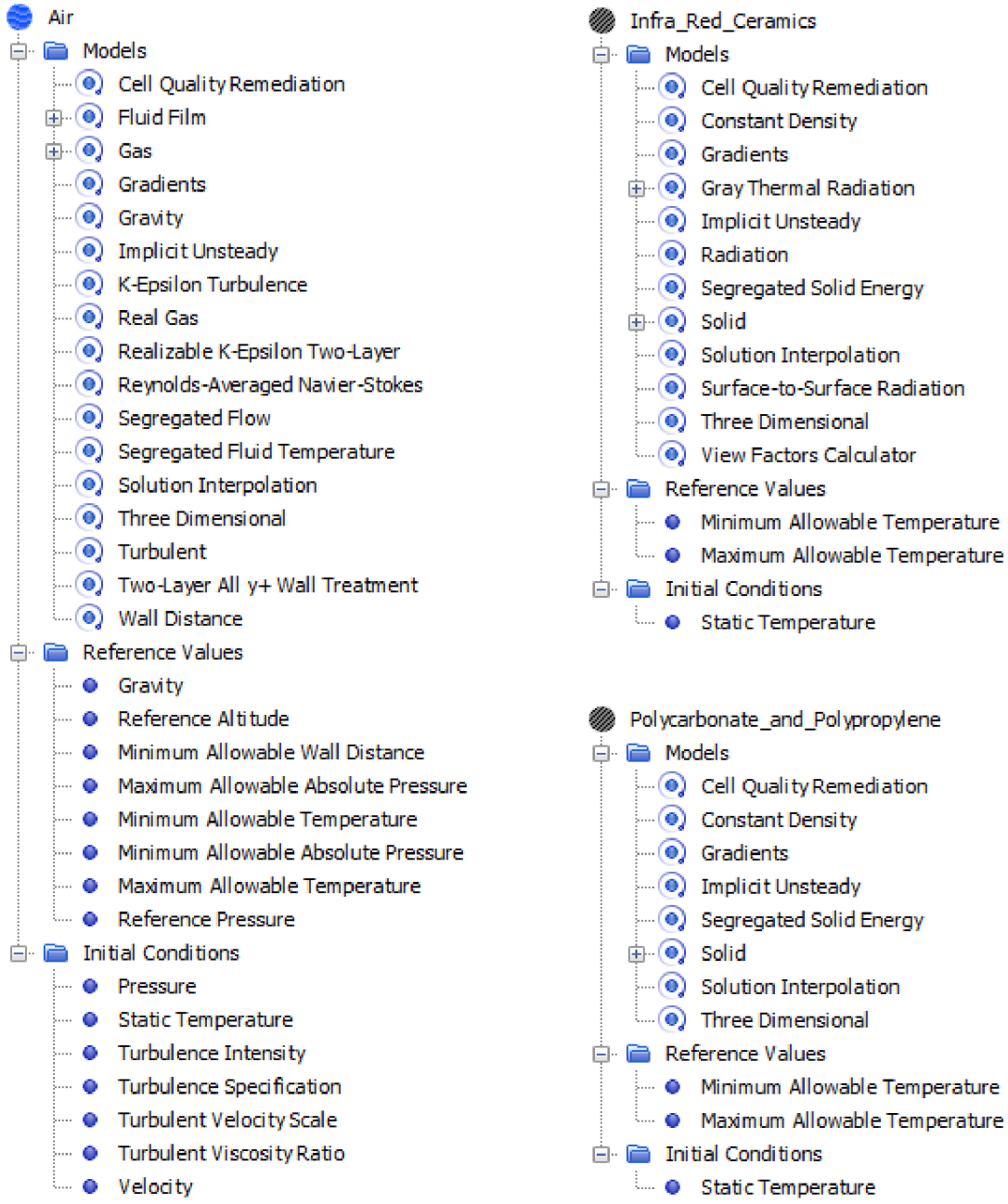

Figure 7.9. Models from simulation tree

Reference values, initial conditions, and material properties (gas and solid models) were defined in previous chapters. In addition, other models were selected so that the simulation corresponds to real conditions as close as possible. In the instance of air, it is a turbulent flow and real gas model, which are solved by Navier-Stokes's equations. For IR ceramic element grey thermal radiation model was chosen (see chapter 2.3 Radiation).

7.1.5 Focus on the fluid film model

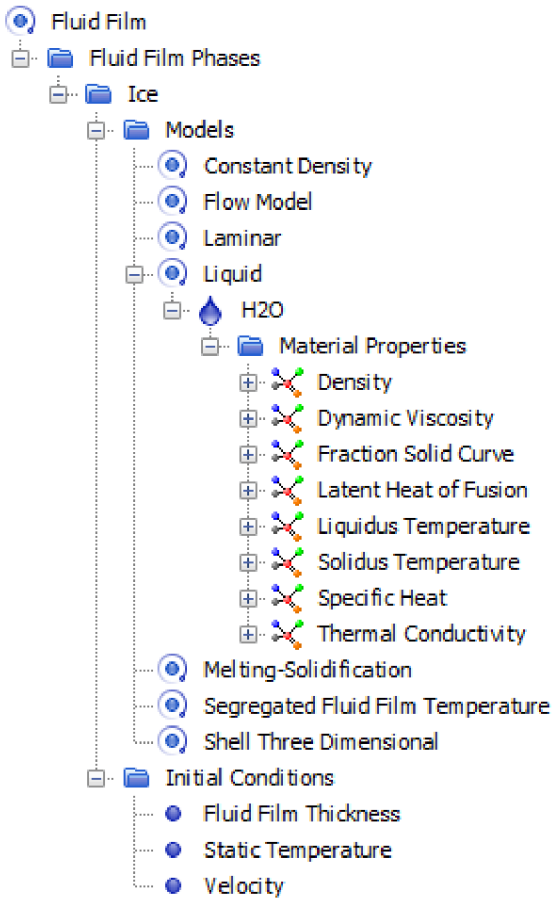

Figure 7.10. Fluid film model in simulation tree

During melting-solidification process dual composition mixture appears, which is composed of two phases – ice (solid medium) and water (liquid medium). Fluid film model works by default with single component phase properties – water (liquid medium) – neglecting different properties of solid phase.

Ice layer thicknesses used in test simulations are in the order of millimetres (maximum ice layer thickness 2 mm) and for these small thicknesses, some fluid film material properties (see figure 7.10.) are not changed distinctively during melting-solidification process. The group contains density, specific heat and thermal conductivity, whose change in area of latent transformation (see chapter 3: Specific latent heat) is negligible and have practically no impact on final solution or simulation stability. These parameters may be set in the simulations as the constant values.

Ice in simulation is considered to be made from pure water and does not contain any admixtures that could affect liquidus and solidus temperature, so both values are at the freezing point of water 273.15 K.

Table 7.3. Material properties for the fluid film model

Fluid Film	H_2O	Material Properties	Density [kg . m^{-3}]	999.84
			Dynamic Viscosity [Pa . s]	Field function
			Fraction Solid Curve [-]	Linear
			Latent Heat of Fusion [J . kg^{-1}]	334000.0
			Liquidus Temperature [K]	273.15
			Solidus Temperature [K]	273.15
			Specific Heat [J . kg^{-1}. K^{-1}]	4181.72
			Thermal Conductivity [W . m^{-1}. K^{-1}]	0.561

The main problem for the fluid film model is dynamic viscosity, which changes drastically when ice starts to melt. Simcenter Star CCM+ assumes constant dynamic viscosity by default which leads to very unstable behaviour causing simulations to diverge not to mention completely unrealistic nature of such approach. The dynamic viscosity parameter therefore had to be refined on the basis of the liquid and solid phases.

Constant dynamic viscosity had been replaced by field function depending on relative solid volume fraction (RSVF) in liquid-solid mixture. Relative solid volume fraction factor represents the amount of solid structure and this function is naturally implemented in Simcenter Star CCM+. Then field function based dynamic viscosity of liquid-solid mixture is: [18]

$$\text{Dynamic viscosity: } \frac{1\,.\,10^{8}\,.\,8.8871\,.\,10^{-4}}{(1-\text{RSVF})\,.\,10^{10}+\text{RSVF}\,.\,8.8871\,.\,10^{-4}} \tag{8}$$

- RSVF is the relative solid volume fraction [-]

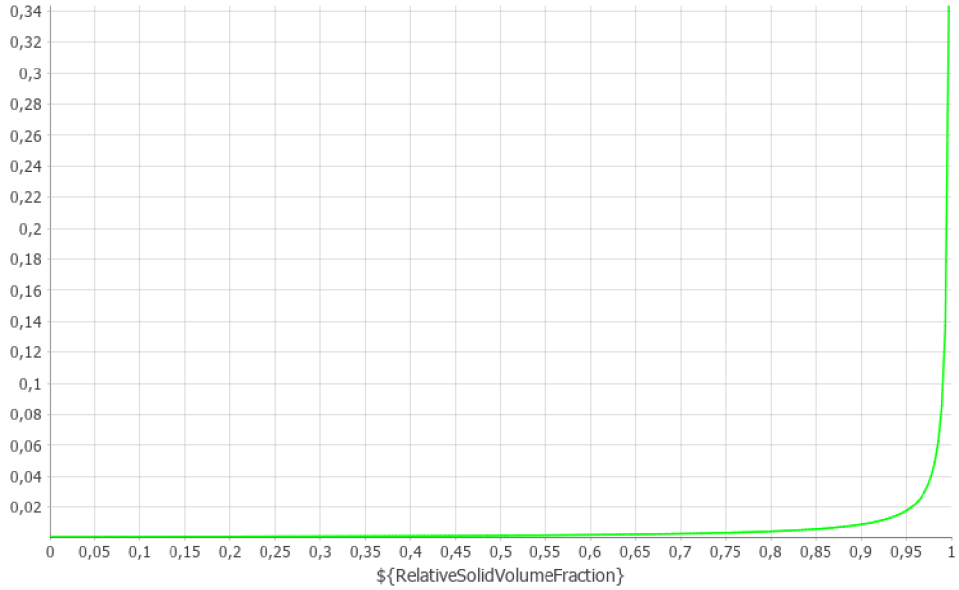

Figure 7.11. Dynamic viscosity set by field function

8 DE-ICING SIMULATIONS

For testing simulations, initial temperatures slightly below freezing point of water as initial condition were set to speed-up simulations. Part when ice layer is heated up but there is still no melting has been neglected as insignificant phase as the aim was to investigate the process of phase transformation of ice layer into water. For simulations the double precision instead of single precision version was used to ensure higher simulation stability (see chapter 5.4 Solvers: Single and double precision).

8.1 Simulation stability

The Courant number can be used in Computational Fluid Dynamics (CFD) simulations to evaluate the transient simulation time step requirements for a given mesh size and flow velocity. Generally, it indicates how much information travels (u) across the mesh cells (Δh) per unit of time (Δt). If the Courant number is more than one, the information is disseminated at each time step by more than one mesh cell, thus making the solution inaccurate and potentially leading to nonphysical results or solution deviations [42].

Generalized Courant number formula: $$C = \frac{u \,.\, \Delta t}{\Delta h} \tag{9}$$

- u is magnitude of the flow velocity [m . s^{-1}]
- Δt is time step [s]
- Δh is characteristic size of the mesh cell [m]

According to Courant number formula simulation stability and accuracy is dependent on the mesh parameters, the velocity of the flow and the time step. Mesh parameters are described in the chapter 7.1.3. and they will not be changed. In our research we used empirical approach where time step was considered as an important parameter affecting computational time and simulation stability was watched and evaluated based on fluid film (ice layer) properties behaviour in time.

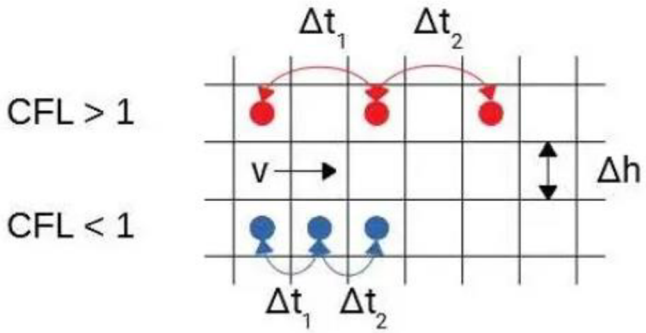

Figure 8.1. The Courant number in the computational mesh [42]

8.1.1 Stable simulations

The main parameter which is monitored and assessed to judge simulation stability is the fluid film thickness and the temperature. Firstly, the thickness expresses the most important information about de-icing, and secondly, it serves as a parameter for simulation stability and convergence. For the fluid film thickness figures 8.2. and 8.3. represent stable simulation plots. Maximum, minimum, and average fluid film thickness monitors give the same value (an initial ice layer thickness) until the point of sufficient energy abundance in the simulation to start the process of melting.

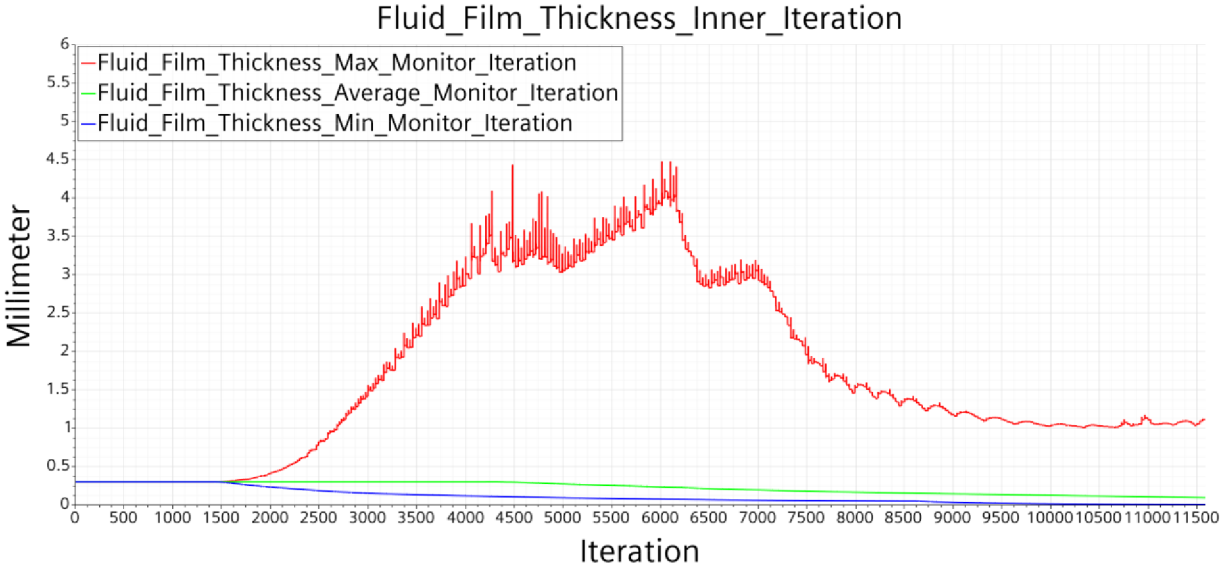

Figure 8.2. Fluid film thickness in the stable simulation (inner iteration plot)

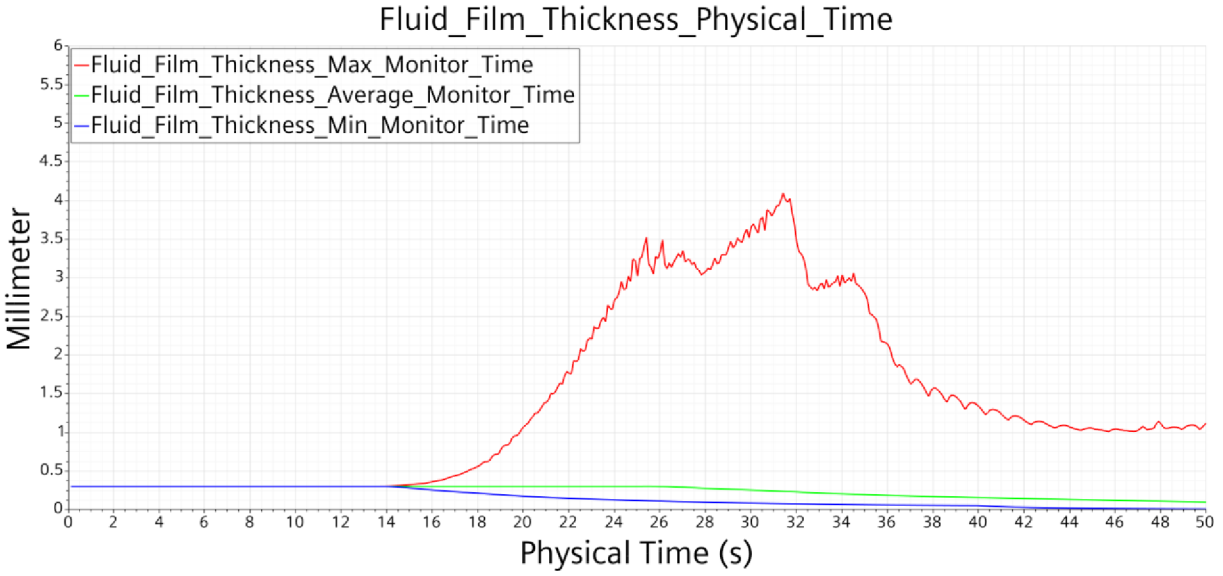

Figure 8.3. Fluid film thickness in the stable simulation (physical time plot)

In figures 8.4. and 8.5. stable fluid film temperature plots are shown. The temperature rises from the initial ambient temperature up to 0 degree Celsius, then comes the latent transformation (see chapter 3: Specific latent heat). From perspective of inner iteration plot, increasing deviations occur, which are caused by energy accumulation in the fluid film (ice layer) during transformation phase. The temperature of the fluid film will not increase in this moment as, energy is absorbed by melting changes of the phase from solid to liquid hence it stays at the constant temperature.

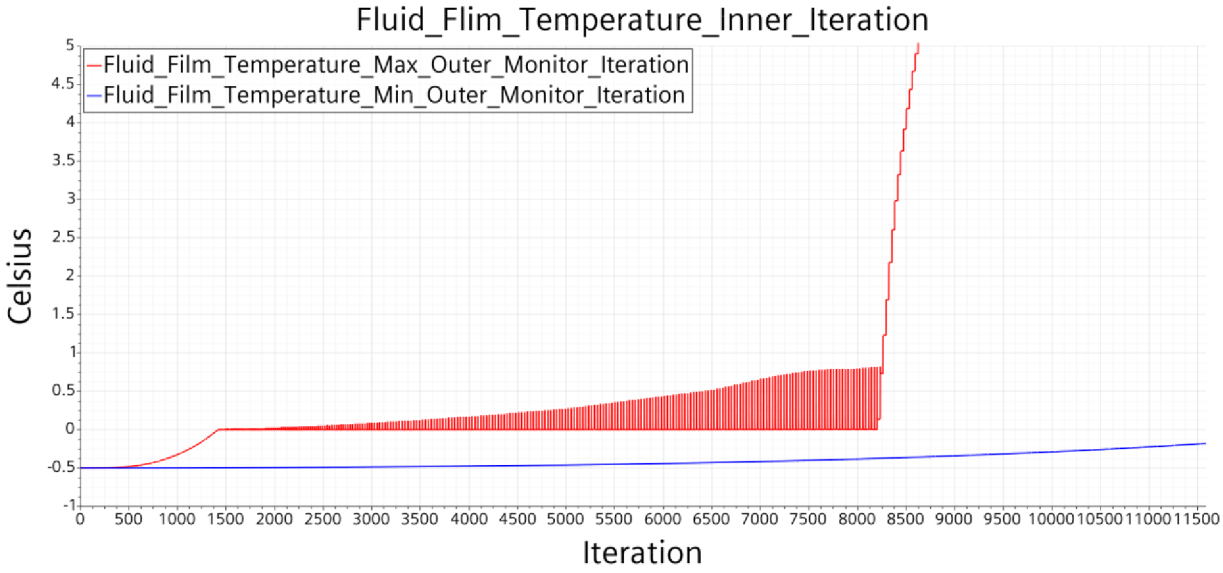

Figure 8.4. Fluid film temperature in the stable simulation (inner iteration plot)

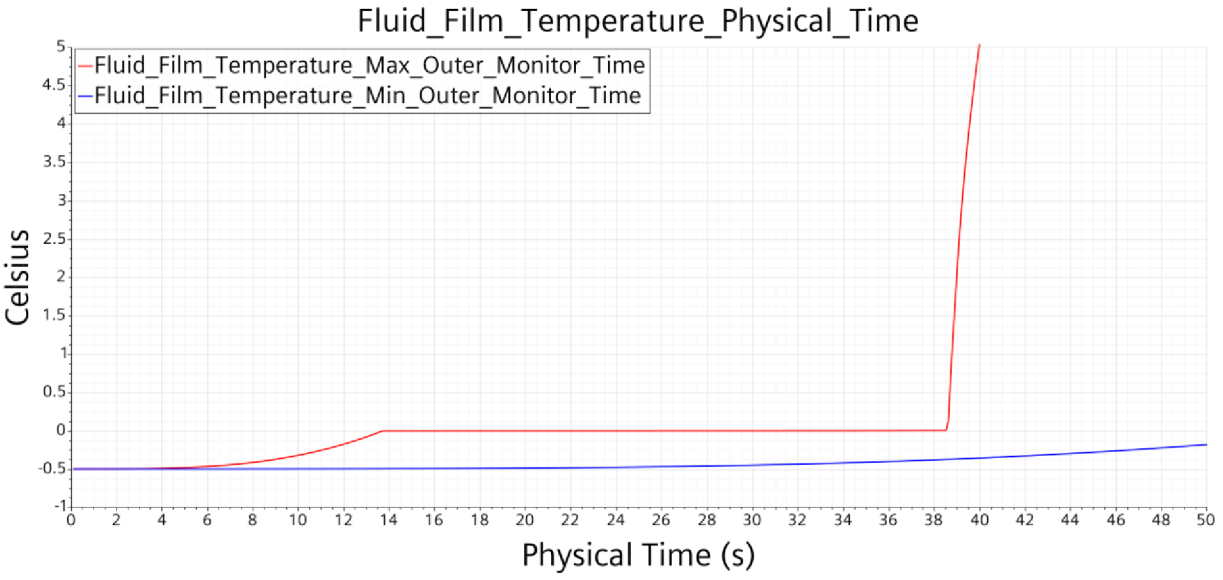

Figure 8.5. Fluid film temperature in the stable simulation (physical time plot)

8.1.2 Fluid film thickness divergency

We have observed that simulations become unstable with increasing the time step. Increasing time step at first affects plot for the fluid film thickness, fluid film temperature plot stays stable as can be seen in the figures 8.4. and 8.5. Increasing ice layer thickness during melting-solidification process causes that values for fluid film thickness climb up to unrealistic high values, see figure 8.6.

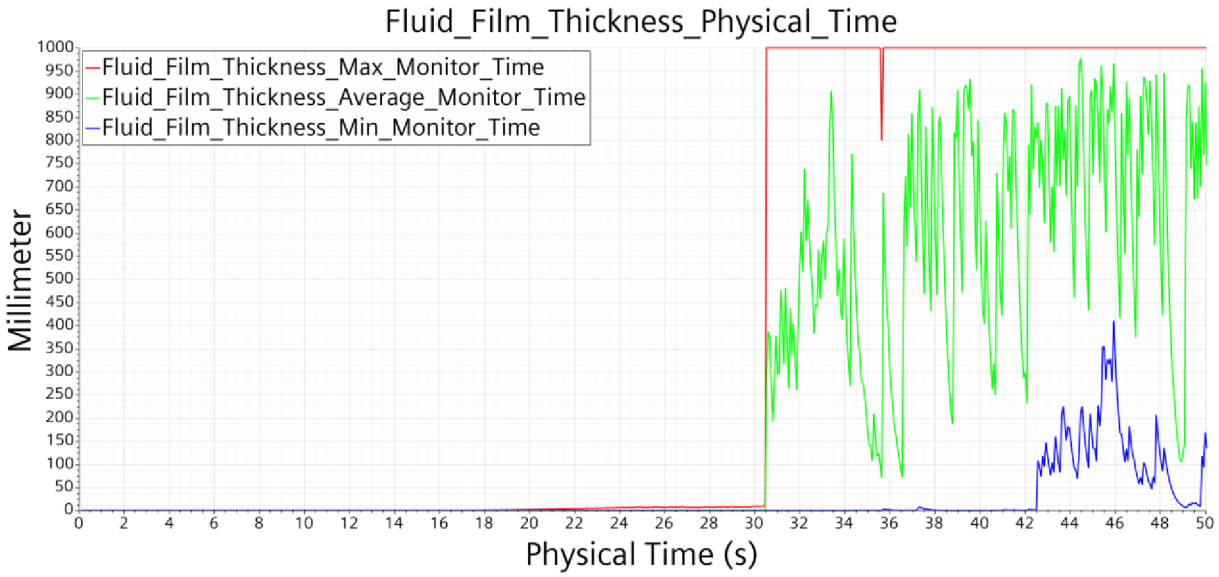

Figure 8.6. Fluid film thickness divergency (physical time plot)

The problem with unrealistically high values can be solved by implementing maximum film thickness parameter, which can be set in a fluid film flow model. The parameter removes any superfluous material above set value from the simulation and improves its stability. Simulation with limited maximum film thickness is shown in figure 8.8.

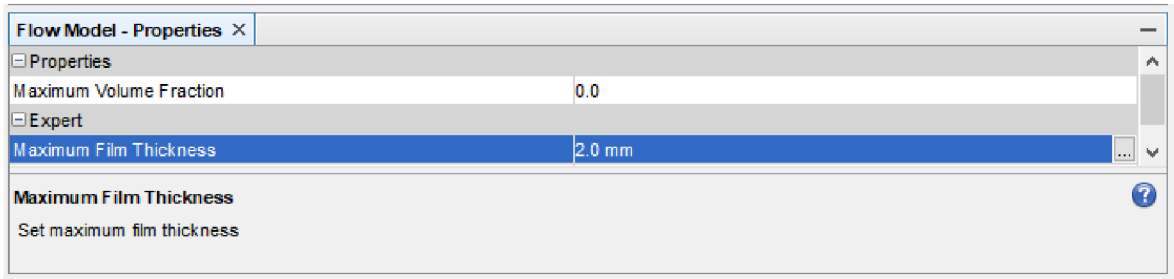

Figure 8.7. Set value for the maximum film thickness

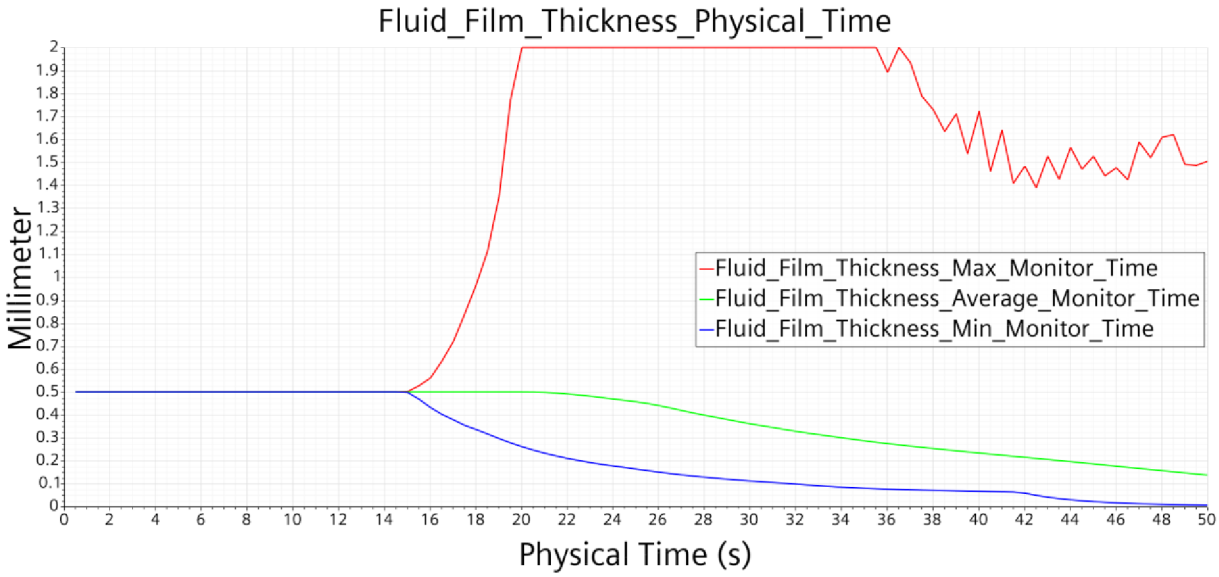

Figure 8.8 Stable simulation with limited maximum film thickness (physical time plot)

Curves for average and minimum fluid film thickness are practically same as for the stable simulations, difference is in the maximum film thickness curve. This curve grows up to value set in maximum film thickness parameter, then this parameter does not allow further growth and the curve stabilizes at a maximum value.

Constraint by the maximum film thickness parameter allows simulation time step to be increased until deviations in the fluid film temperature plots occurs. The temperature plot deviations are described in the next chapter.

8.1.3 Fluid film temperature deviations

Fluid film thickness limitation allows to use longer time steps, but the time step cannot be increased to infinity value as time step increase affects stability of the simulation which can easily be observed in fluid film temperature plots.

We have observed two different behaviours of fluid film temperature plots:

a) Inner iteration structure of fluid film temperature corresponding to plausible solution

b) Inner iteration structure of fluid film temperature causing unrealistic results

a) Inner iteration structure of fluid film temperature corresponding to plausible solution

In comparison to the temperature plot observed with low time steps in the figure 8.4. deviations in latent heat transformation appears. The deviations appear only in the inner iteration plot, in physical time plot there are no changes compared to stable temperature plot in the figure 8.5. Due to this fact the calculations were stable, and u achieved a converged solution (results do not contradict logical assumptions), but its settings are on the limit of possibilities.

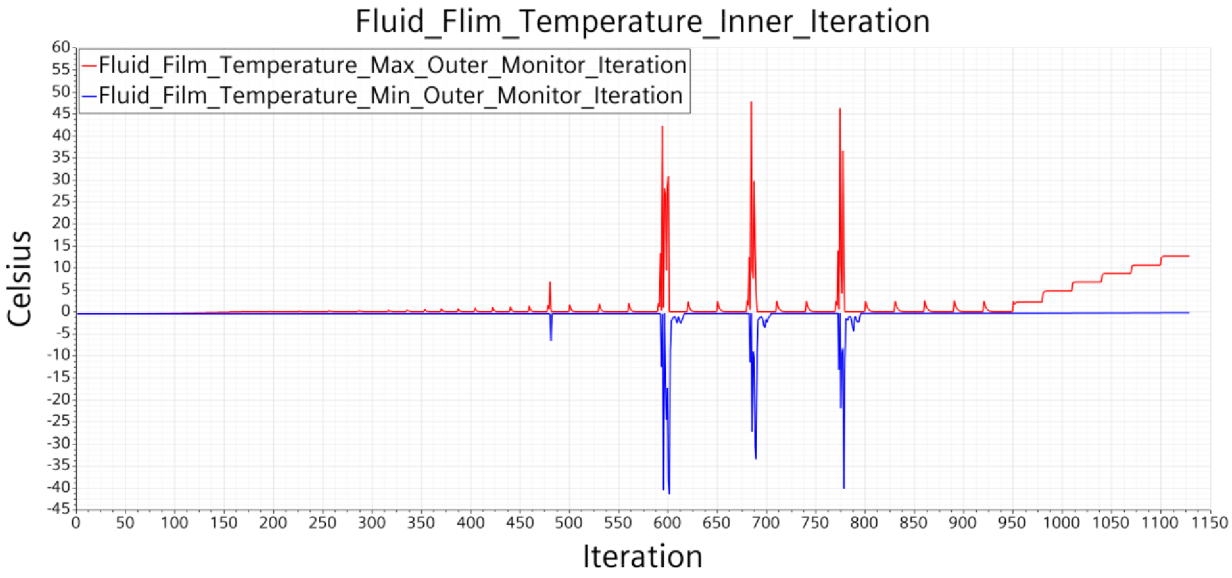

Figure 8.9. Fluid film temperature deviation still leads to plausible solution (inner iteration)

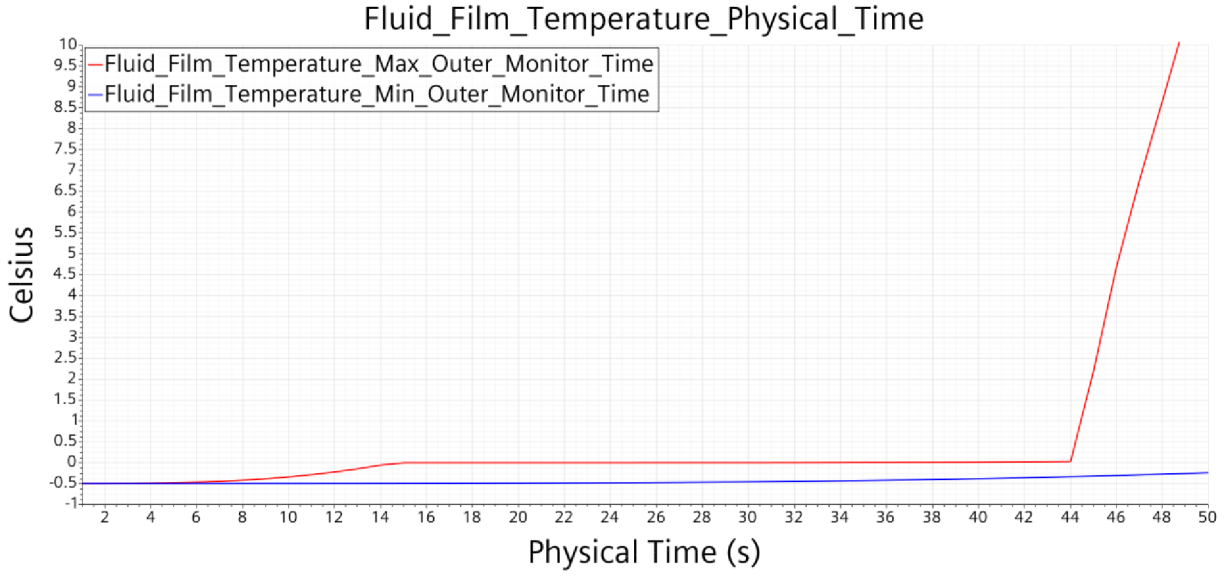

Figure 8.10. Fluid film temperature deviation still leads to plausible solution (physical time plot)

b) Inner iteration structure of fluid film temperature causing unrealistic results

With further time step increase more deviations occur in temperature plots. The deviations gain higher values and solver is unable to calculate realistic results. Deviations are also visible in the physical time plot and simulations with such a course cannot be taken as credible (it is not possible to get lower temperatures than initial ambient temperature).

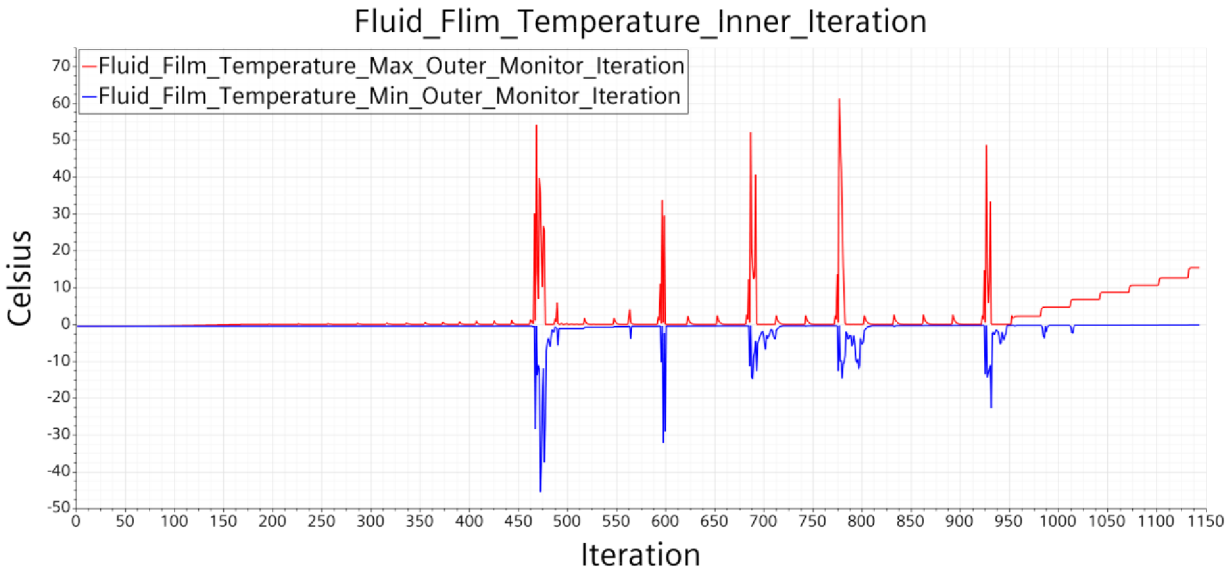

Figure 8.11. Fluid film temperature deviation causes unrealistic results (inner iteration)

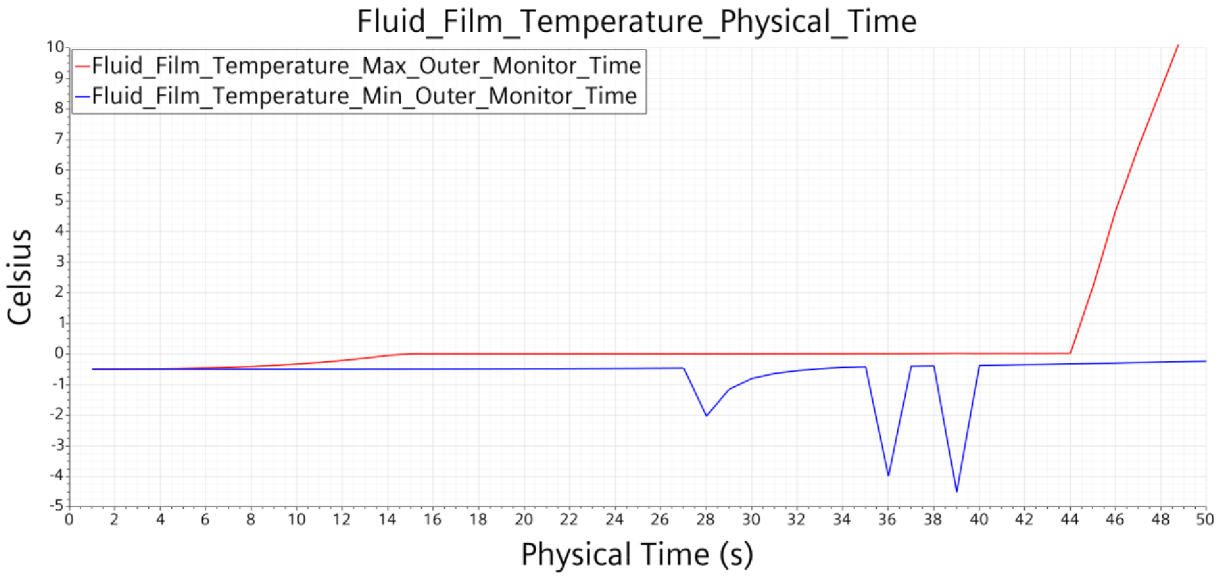

Figure 8.12. Fluid film temperature deviation causes unrealistic results (physical time plot)

8.2 Data collection

Considering various behaviour of de-icing simulations, we have seen, from stable to completely unstable and diverging simulations, the main aim was to find simulation stability region varying three different parameters which have been shown to be the most important ones in practical applications, namely:

- Initial ice layer (fluid film) thickness
- Time step
- Maximum film thickness limit

For that purpose, a particular combination of a specific time step, initial fluid film thickness and maximum film thickness limit was chosen for each simulation. In total, for research in this master's thesis more than 1 600 simulations were performed. In order to prepare, run and post-process such a number of simulations further optimizations (apart from simplifying of the simulation model and setting initial conditions to be close to melting point) were required – automation by means of java macro was designed and applied. An example of the code automizing numerical tests with different time step sizes can be found in the appendix A.

8.3 Evaluation

The evaluation was carried out with the help of Microsoft Excel. Every simulation result was processed into a table and then assessed whether it:

- is stable from all perspectives
- has a deviation in fluid film temperature plot on inner iterations level
- or is unstable and gives unrealistic results.

At first, simulations for individual fluid film thicknesses were evaluated, then the data for all thicknesses were combined into 3D graphs which contains all the information.

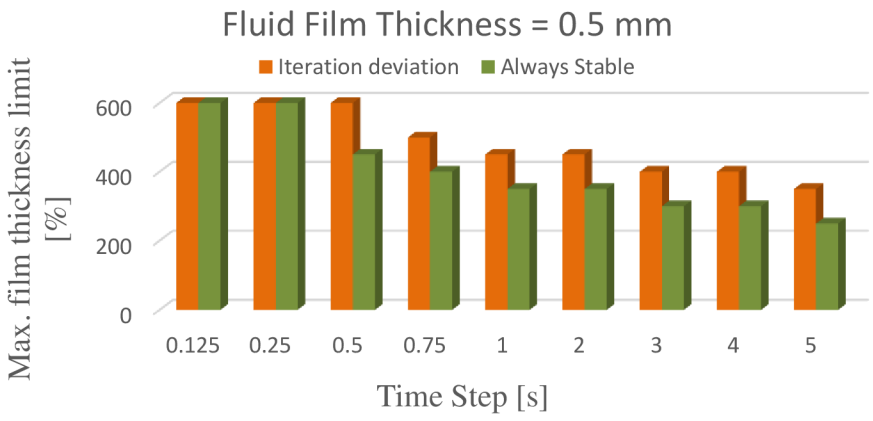

Figure 8.13. Individual evaluation for simulations with fluid film thickness 0.5 mm

8.3.1 Simulations without limited maximum film thickness

Each one simulation is represented by a point in the graph below. Green points are simulations with convergent solution and represent stable simulations from chapter 8.1.1. For these simulations, maximum film thickness parameter was disabled, due to this fact short time steps were required for a stable solution. For longer time steps fluid film thickness exceeds stability border and simulation becomes unstable (see figure 8.6.), these simulations are represented by red points.

Initial fluid film thickness [mm]	0.1	0.2	0.3	0.4	0.5	0.6	0.7	0.8
Maximum time step [s]	2.2	0.7	0.28	0.07	0.05	0.044	0.02	0.018

Initial fluid film thickness [mm]	0,9	1,0	1,2	1,4	1,6	1,8	2,0
Maximum time step [s]	0.015	0.011	0.01	0.009	0.008	0.007	0.006

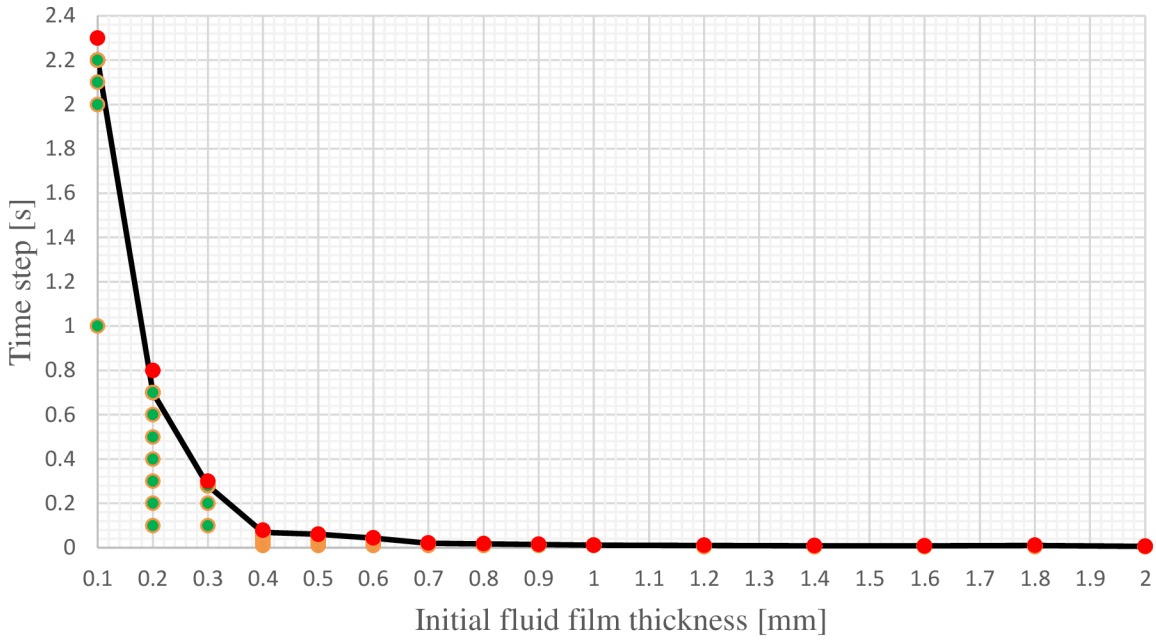

Figure 8.14. Convergence window (under the curve) for simulations with no limited maximum film thickness

It is important to note that figure 8.14. is valid for the model used in testing simulations. For real headlamp application the graph may take a slightly different course, which is primarily dependent on the headlamp geometry, further on the heat source nature and temperature distribution in the system. For complicated cover lens shapes, accumulated water might be resulting in dripping drops and this leading to local increase of fluid film thickness. As mentioned in previous chapter, fluid film model relates to a shell region with physically zero thickness and too rapid increase of fluid film thickness causes instabilities in implemented solver. Appropriate time step for simulations with no limited maximum film thickness is therefore dependent also on the individual model and conditions for water accumulation.

8.3.2 Simulations with limited maximum film thickness

Simulations with limited maximum film thickness have been processed into 3D graph (see figure 8.8.). The maximum film thickness limitation is given by percentage of initial fluid film thickness (ice layer), so the limitation is dependent on the individual fluid film thickness.

Green colour represents a stable solution for fluid film temperature plots (see figures 8.4. and 8.5.), that means, in the solution there are not any deviations from perspective of inner iteration plots which could affect simulation stability. Any setting from the area below the surface guarantees a stable simulation and relevant results. For thin fluid film it is not necessary to strictly limit the maximum film thickness, the simulation is stable for any time step. For thick fluid films the situation is opposite, short time steps and a strict limit for maximum film thickness must be set to obtain a stable solution. The red area represents that there is not simulation setting without deviations on temperature inner iteration level. For bigger time steps it is not possible to get solution without deviations from perspective of temperature inner iteration.

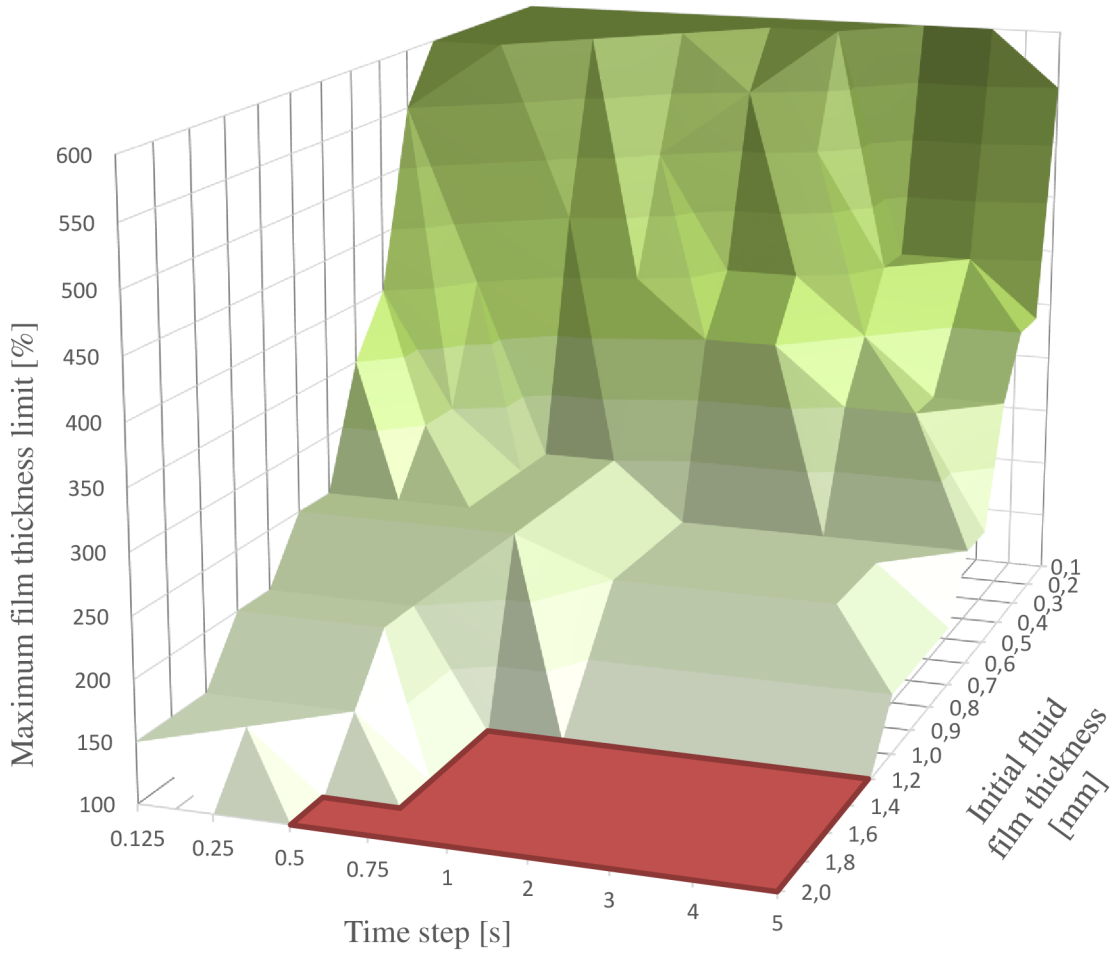

Figure 8.15. Always stable 3D convergence window for simulations with limited film thickness

In the figure 8.16. stability from perspective of temperature inner iterations is plotted.

The area below the orange and above green surfaces represents simulation setting with deviation from perspective of fluid film temperature on inner iteration level, which still leads to plausible solution (see figures 8.9. and 8.10.). From perspective of physical time plot solution is still stable and can be taken as realistic. Increased attention needs to be put into simulations with settings close to the orange surface area. Border setting may cause great deviations in fluid film temperature plots on inner iteration level which can appear in the physical time plot as well. Such a simulation becomes unrealistic, so it is recommended use values from more stable area.

Orange surface uncovers interesting area of parameters (compared to figure 8.15. where red area appears) which enables to get stable solution at least on physical time level (although not necessarily on iteration level) which would be otherwise not possible. This is applicable for thicker fluid film thickness when choosing longer time step together with maximum film thickness limit.

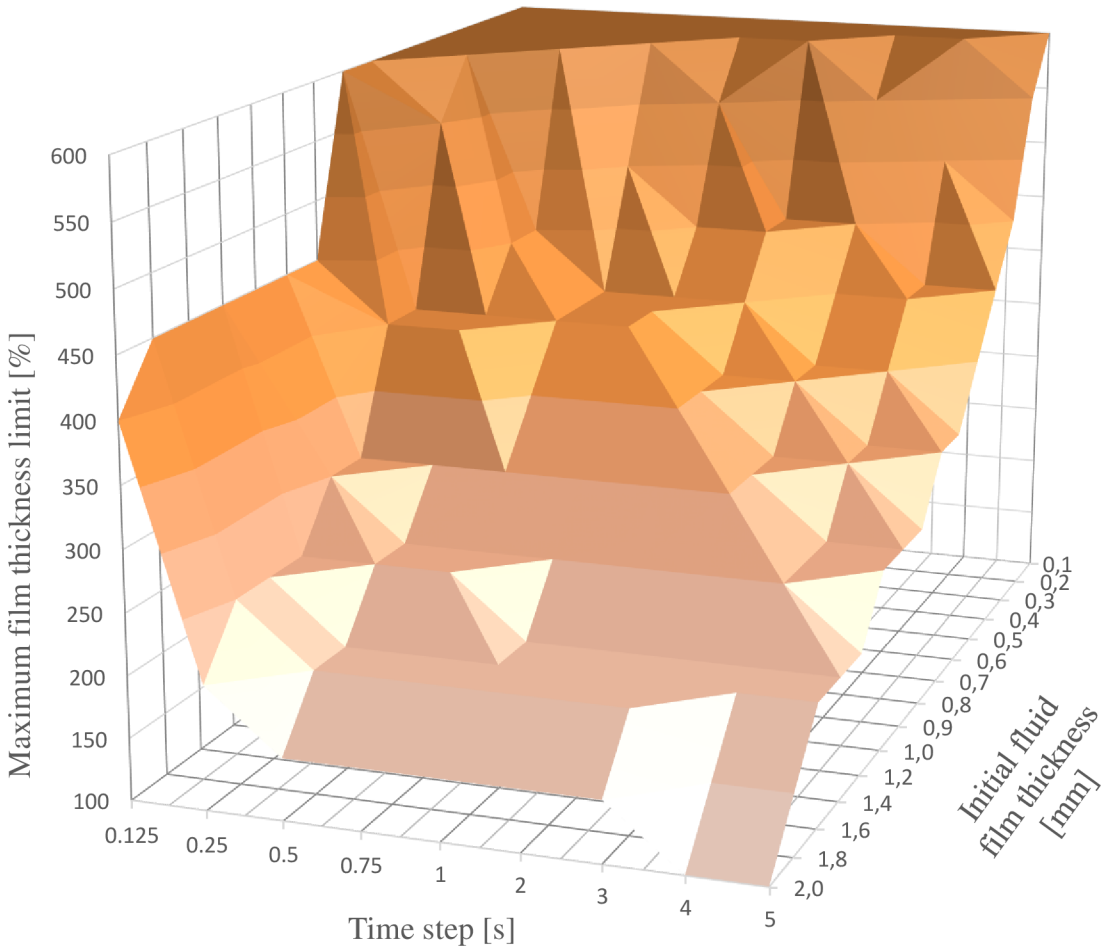

Figure 8.16. Inner iteration deviation 3D convergence window for simulations with limited film thickness

8.4 Computational time saved

Computational times for the simulations with and without limited maximum film thickness turned out to be vastly different. The figure 8.17. shows the comparison between stable simulations with and without limited maximum film thickness and axis *time saved* represents how many times is the simulation with limited maximum film thickness faster than simulation without this feature. Individual colours represent maximum film thickness limits for the maximum film thickness parameter, the higher maximum film thickness limit, the better the resolution of the simulation (less melted water is removed from the simulation). It is up to the simulation expert to decide which setting is the best, it is possible to solve simulations with strict limitation and less accuracy in short time, or vice versa.

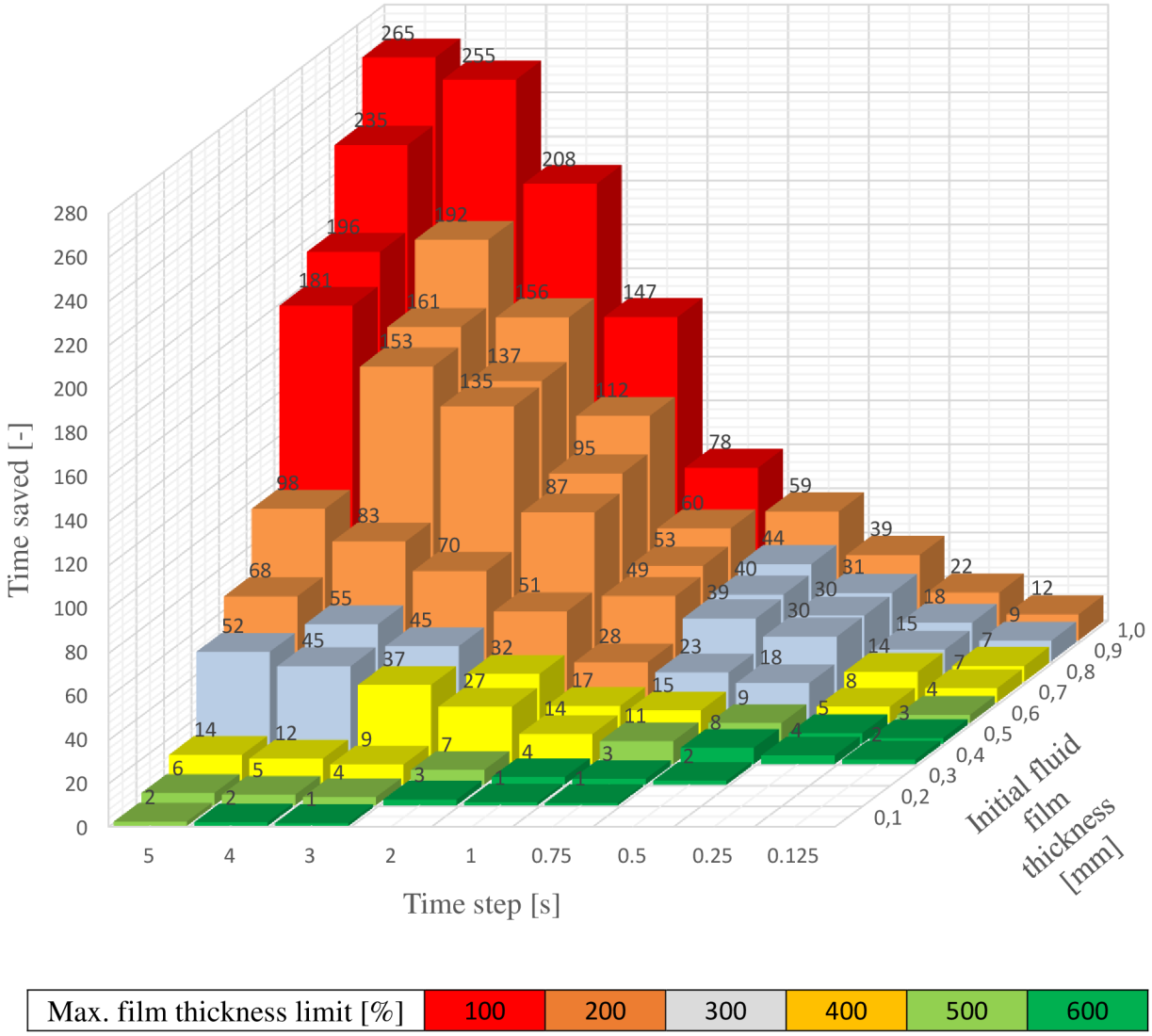

Figure 8.17. Time saved by maximum film thickness limitation (initial ice layer thickness from 0,1 to 1 mm)

9 DE-ICING MODEL USED FOR CAR HEADLAMP

Fluid film simulations of de-icing are primarily designed for truck headlamps, which are operated in challenging climatic conditions (blizzards and low temperatures causes headlamp cover lens icing). Headlamps for these trucks are still in development and their designs is confidential, so they cannot be used as background CAD model in this master's thesis.

Simulation model works for any headlamp de-icing, for illustration real headlamp was used as background for the simulation experiments. Inside the headlamp H4 light bulb is used and represents heat source. Ice layer 0.5 mm on outer side of the headlamp cover lens and temperature minus 10 degree of Celsius were set as initial conditions and results of two de-icing simulations with different parameters are presented in this chapter.

9.1 Simulation setting without limited maximum film thickness

For this simulation low time step had to be used to achieve stable convergent solution, otherwise increasing fluid film thickness (due to flowing down drops) causes the system divergency and invalid solution. Maximum time step for the simulation with no limited maximum film thickness can be found in the chapter 8.3.1. For stable convergent solution for ice layer thickness 0.5 mm maximum time step 0.05 s had to be set, for larger time steps simulation diverged. This setting is relevant for the simple model which is described in the chapter 7.1., for real headlamp with more complicated cover lens geometry allows water accumulation (fluid film thickness increasing), even lower time steps had to be used. Experimentally it was found that time step 0.01 s must be set in the simulation for the convergent solution.

9.2 Simulation setting with limited maximum film thickness

For this simulation maximum film thickness parameter is enabled, that means, value for the maximum film thickness is set by the user in the simulation. This parameter activates function, which removes excess material over the limit from the simulation as well as the simulation becomes stable for larger time steps in comparison to previous option (absence of accumulating water in flowing down drops improves system stability). Border convergence setting for the simulations with limited maximum film thickness can be found in the chapter 8.3.2. Maximum time step depends on the fluid film thickness limitation, the bigger the limitation the higher time step could be used. Optimal parameter selection depends usually on requirements. For quick estimation of de-icing behaviour large time steps with big maximum film thickness limitation should be used (short simulations), for detailed simulations capturing all 'high-resolution' effects setting is reversed (long simulations). For demonstration, simulation with time step 2 s and maximum film thickness limitation with 500 percent of initial ice layer thickness was used (limitation by 1.5 mm).

9.3 De-icing performance

Differences between simulations mentioned in chapters 9.1 and 9.2 will be discussed in this chapter. To compare both simulation results the same range for fluid film thickness scalar field was set 0.05 mm (minimum) and 1.5 mm (maximum). Figure 9.1. shows the comparison with simulations employing limited maximum film thickness on the left side and simulations lacking this parameter on the right side.

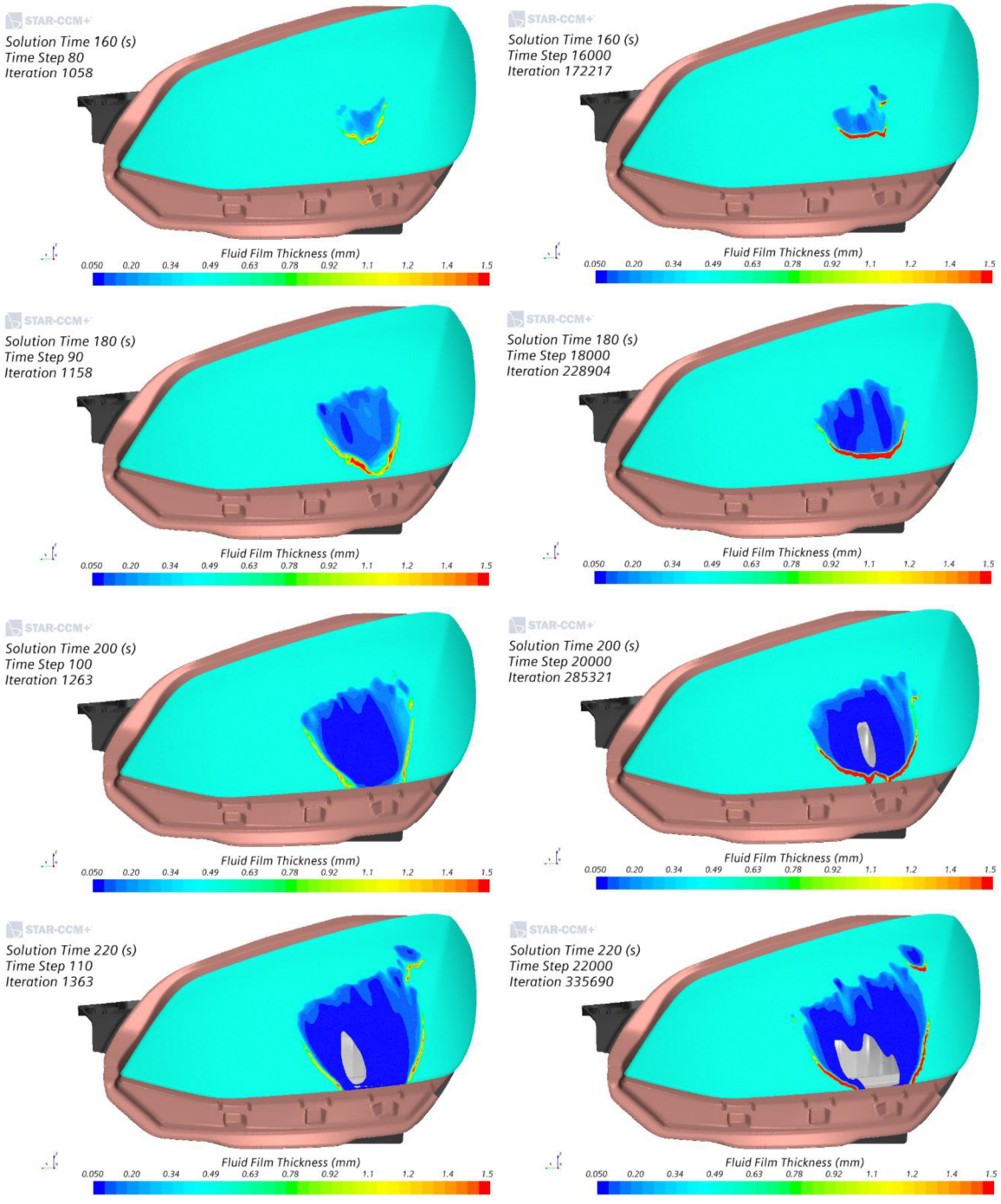

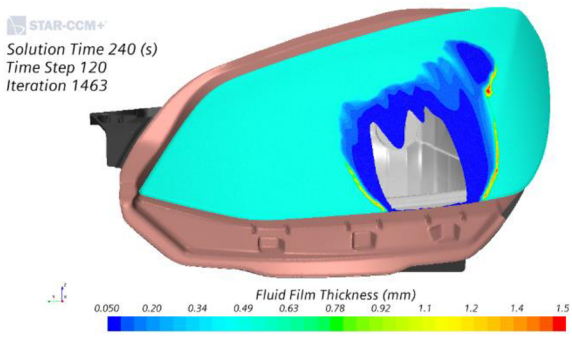
STAR-CCM+
Solution Time 240 (s)
Time Step 120
Iteration 1463
Fluid Film Thickness (mm)
0.050 0.20 0.34 0.49 0.63 0.78 0.92 1.1 1.2 1.4 1.5

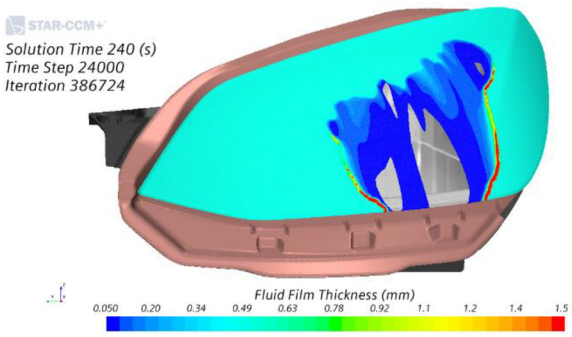
STAR-CCM+
Solution Time 240 (s)
Time Step 24000
Iteration 386724
Fluid Film Thickness (mm)
0.050 0.20 0.34 0.49 0.63 0.78 0.92 1.1 1.2 1.4 1.5

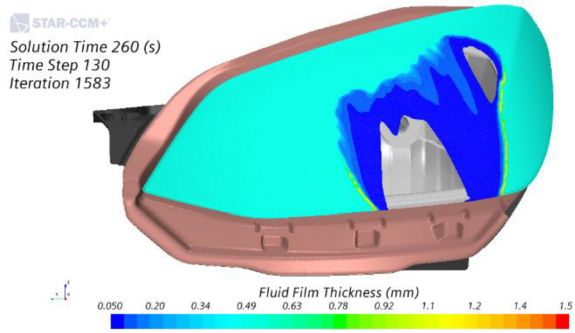
STAR-CCM+
Solution Time 260 (s)
Time Step 130
Iteration 1583
Fluid Film Thickness (mm)
0.050 0.20 0.34 0.49 0.63 0.78 0.92 1.1 1.2 1.4 1.5

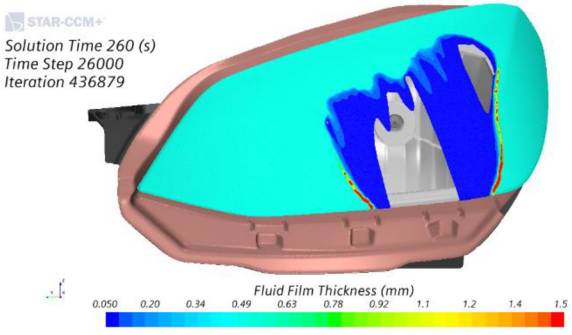
STAR-CCM+
Solution Time 260 (s)
Time Step 26000
Iteration 436879
Fluid Film Thickness (mm)
0.050 0.20 0.34 0.49 0.63 0.78 0.92 1.1 1.2 1.4 1.5

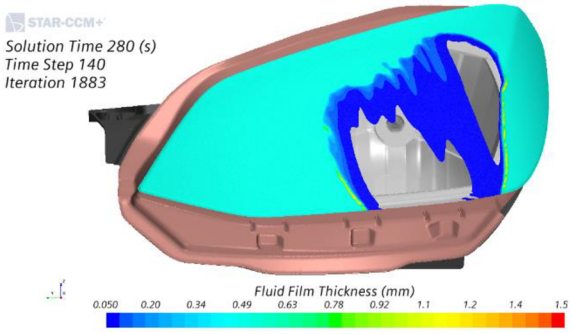
STAR-CCM+
Solution Time 280 (s)
Time Step 140
Iteration 1883
Fluid Film Thickness (mm)
0.050 0.20 0.34 0.49 0.63 0.78 0.92 1.1 1.2 1.4 1.5

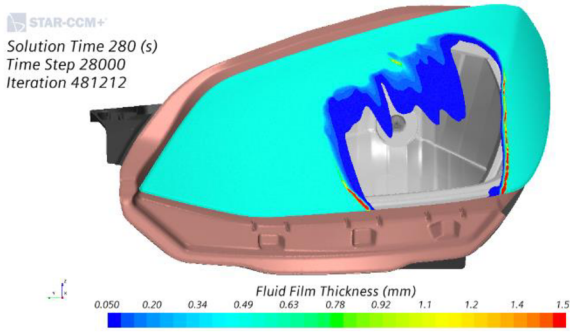
STAR-CCM+
Solution Time 280 (s)
Time Step 28000
Iteration 481212
Fluid Film Thickness (mm)
0.050 0.20 0.34 0.49 0.63 0.78 0.92 1.1 1.2 1.4 1.5

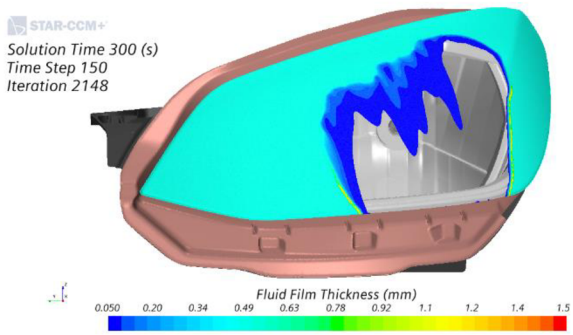
STAR-CCM+
Solution Time 300 (s)
Time Step 150
Iteration 2148
Fluid Film Thickness (mm)
0.050 0.20 0.34 0.49 0.63 0.78 0.92 1.1 1.2 1.4 1.5

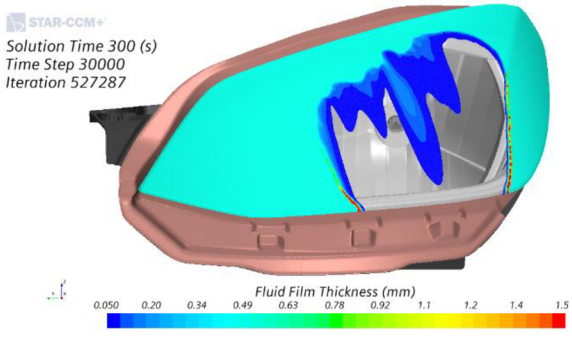
STAR-CCM+
Solution Time 300 (s)
Time Step 30000
Iteration 527287
Fluid Film Thickness (mm)
0.050 0.20 0.34 0.49 0.63 0.78 0.92 1.1 1.2 1.4 1.5

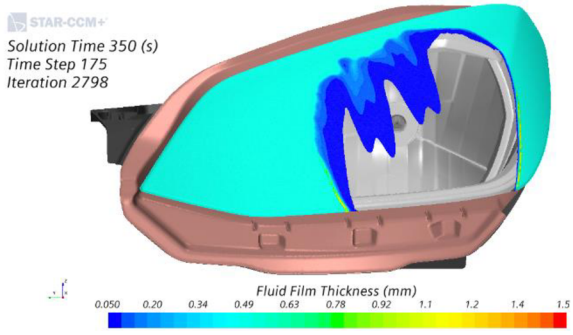
STAR-CCM+
Solution Time 350 (s)
Time Step 175
Iteration 2798
Fluid Film Thickness (mm)
0.050 0.20 0.34 0.49 0.63 0.78 0.92 1.1 1.2 1.4 1.5

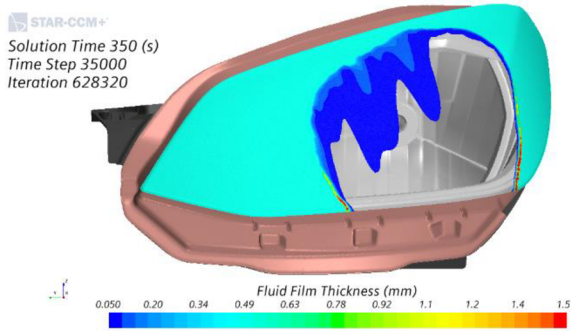
STAR-CCM+
Solution Time 350 (s)
Time Step 35000
Iteration 628320
Fluid Film Thickness (mm)
0.050 0.20 0.34 0.49 0.63 0.78 0.92 1.1 1.2 1.4 1.5

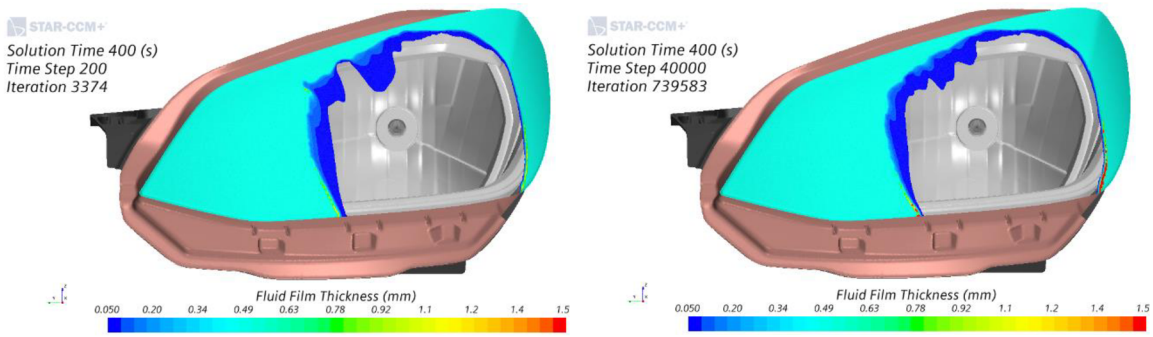

Figure 9.1. Simulations with enabled and disabled limited maximum film thickness

- Conclusion from the perspective of complete simulation

From “macroscopic” scale both simulations show similar course. Physical times when first fluid film changes start to appear are the same (de-icing process starts at the same moment), also emerging (de-iced) dry spots have similar shapes during simulation.

Main difference is in the computational time. For simulation with limited maximum film thickness result is available after 3 hours while in case of the simulation without limited maximum film thickness 320 hours were required to get complete results. Computational time which was saved by employing limited maximum film thickness corresponds with figure 8.17. and is more than 100 times faster than the second one.

This chapter focuses on the complete picture of de-icing performance in both simulations, therefore same minimum and maximum values were set for fluid film thickness scalar field in scenes for both cases. For the second simulation with no limitation of maximum fluid film thickness maximum value 1.5 mm of scalar field does not allow insight into 'high-resolution' effects as real thickness values locally exceed the limit set in the scene. The possibilities which are offered by detailed simulation without limited maximum film thickness are discussed in next chapter.

9.4 Detailed view of de-icing behaviour

For detailed view increased maximum scalar field limit was used. Raising this limit does not affect simulation with limited maximum film thickness in any way, because enabled parameter removes any excess material over the set limit by default.

Maximum scalar field increase has got impact only on visualization of simulation without limited maximum film thickness, where allows to display 'high-resolution' effects. These effects are most visible at the beginning of melting process, where water from locally melted ice accumulates in flowing down drops. Figures in this chapter show the difference between the two simulations mentioned. On the left side are simulations with limited maximum film thickness, right side represents scenes from the simulation with disabled parameter.

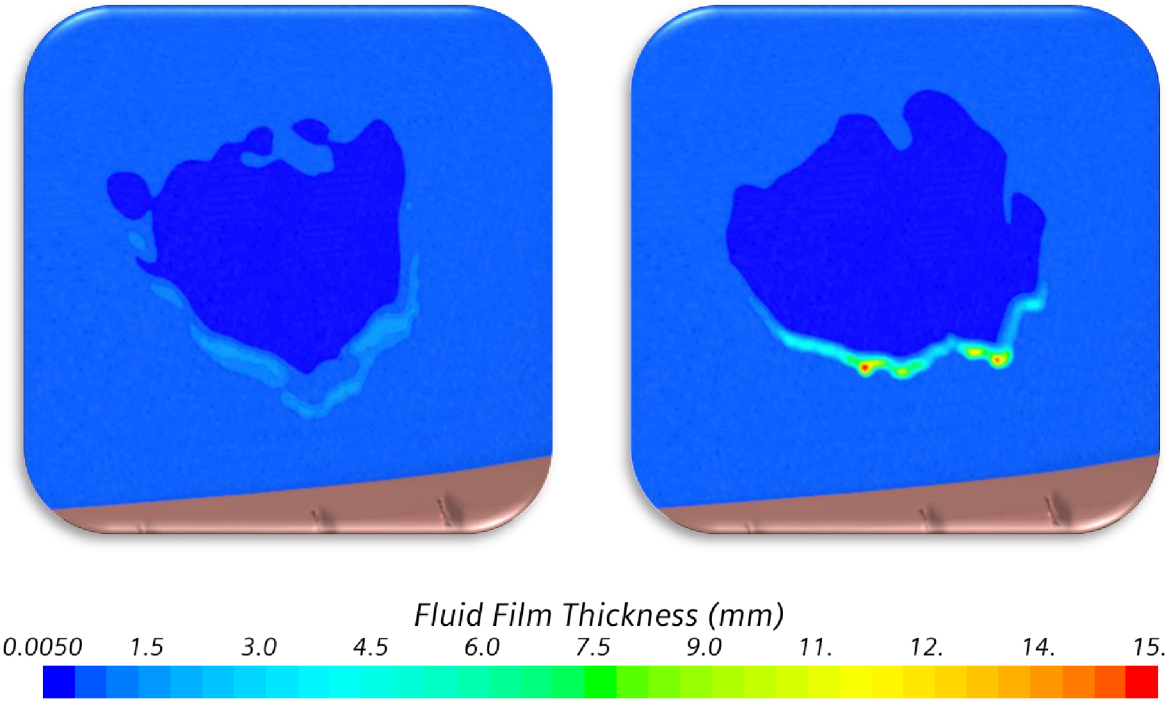

Figure 9.2. Simulations with and without limited maximum film thickness, solution time: 170 s

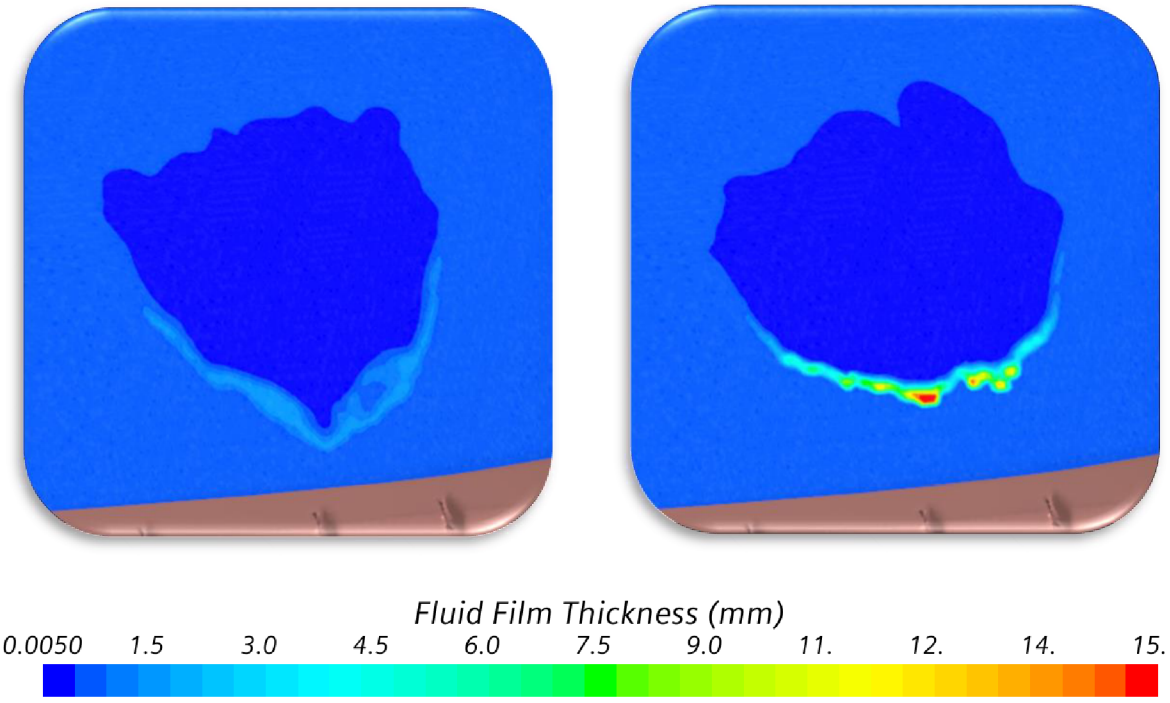

Figure 9.3. Simulations with and without limited maximum film thickness, solution time: 176 s

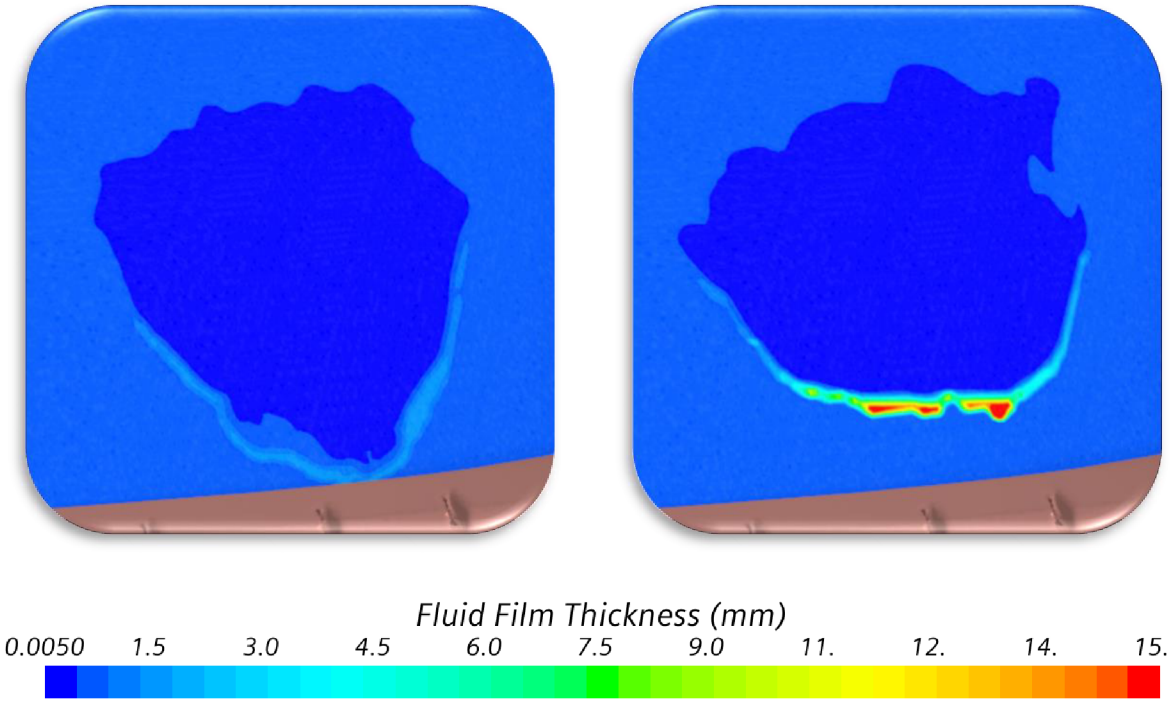

Figure 9.4. Simulations with and without limited maximum film thickness, solution time: 184 s

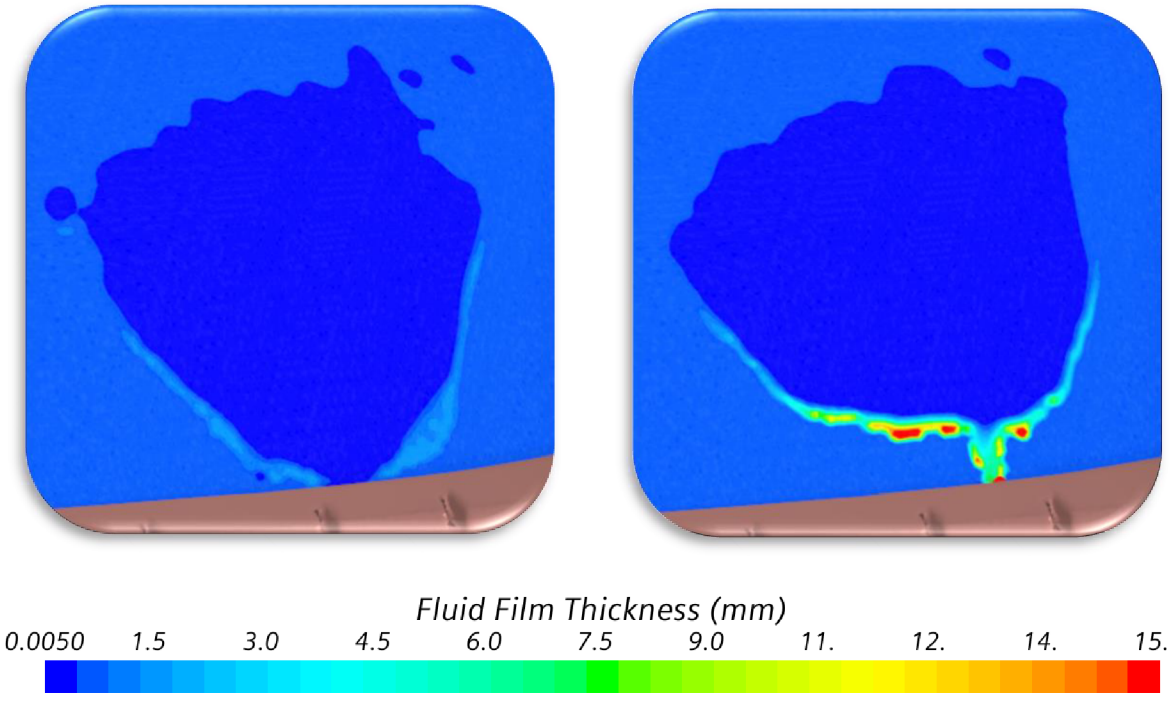

Figure 9.5. Simulations with and without limited maximum film thickness, solution time: 190 s

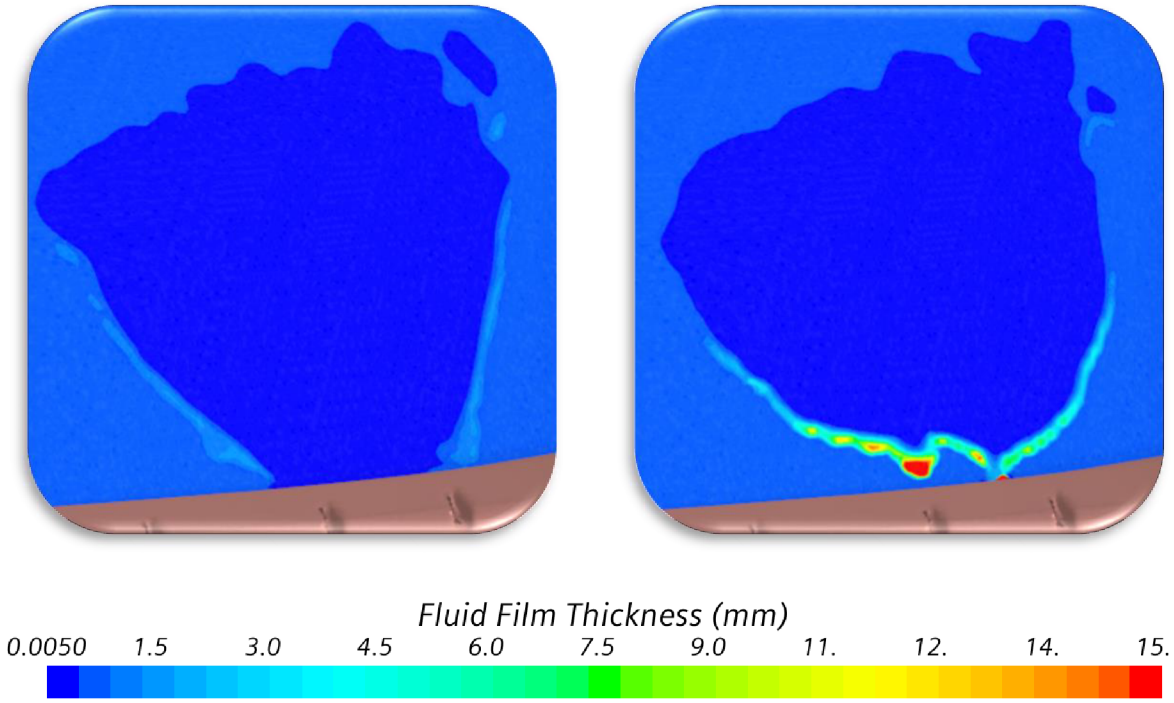

Figure 9.6. Simulations with and without limited maximum film thickness, solution time: 198 s

- Conclusion

Combination of detailed simulation with unlimited maximum film thickness with sufficiently high scalar field maximum in fluid film thickness scene allows to capture and view 'high-resolution' effects in de-icing performance. Due to lower time step resolution, there is possibility in simulation to capture and calculate every flowing down drop at a price of long computational times. On the other hand, the simulation with limited maximum film thickness is not so much detailed because melted water over the maximum film thickness limit is removed from the system and time steps are too large to capture single droplet effects but it offers the same course of de-icing behaviour in considerable shorter computational times.

10 CONCLUSION

Numerical simulations are powerful tools used in the development process. High cost of physical testing can be reduced as simulations can detect problems early in the development process.

Although numerical simulations provide these possibilities, achieving the results can sometimes be time consuming. The computation time is dependent on many parameters that need to be optimized. This master's thesis deals with de-icing simulations that work on the principle of the fluid film model. Time step, maximum film thickness and initial fluid film thickness are assessed parameters and achieving their optimal combination for simulation is the aim of this work this work from perspective of:

- stability and convergence of de-icing simulations
- best choice of transient simulation parameters.

The results presented in thesis are usable for any de-icing application with the fluid film model. For customers or simulation experts detailed de-icing simulations are usually not necessary, the most important output is the time required for de-icing process and emerging dry spots (possibility for light transmission), these parameters indicate roadworthiness of a vehicle. Due to this fact, limited maximum film thickness simulations with low computational times are more suitable for automotive headlamp de-icing applications and research dedicated to optimal parameter choice for de-icing simulations is the content of this master's thesis.

LIST OF USED RESOURCES

1. LED vs. Halogen vs. Xenon: Which is Better for You? CarCareTotal.com [online]. CarCareTotal.com: Amazon Services, 2017 [cit. 2020-07-13]. Dostupné z: https://carcaretotal.com/led-vs-halogen-vs-xenon/
2. POPA, Bogdan. Battle of the Headlights: Halogen vs. Xenon vs. LED vs. Laser vs. Conversion Kits. Autoevolution [online]. autoevolution: SoftNews Net SRL, c2008-2021, 16 Nov 2010 [cit. 2020-07-13]. Dostupné z: https://www.autoevolution.com/news/battle-of-the-headlights-halogen-vs-xenon-vs-led-26530.html
3. BASIC PRINCIPLES OF CAR LIGHTING TECHNOLOGY. Hella.com [online]. Warden, Banbury, Oxon: HELLA GmbH & Co., c2021 [cit. 2020-07-15]. Dostupné z: https://www.hella.com/techworld/uk/Technical/Automotive-lighting/Basic-principles-of-car-lighting-technology-220/
4. LIGHTING THE FUTURE: STANDARD AND HIGH PERFORMANCE AUTOMOTIVE HALOGEN BULBS. Http://www.hella.co.za [online]. Moselville, Uitenhage, SOUTH AFRICA: HELLA Automotive South Africa (Pty), c2021 [cit. 2020-07-15]. Dostupné z: https://www.hella.com/hella-za/assets/media_global/HASA_Bulbs_Catalogue_2012_LRes.pdf
5. Automotive Bulbs. HELLA in New Zealand [online]. New Zealand: HELLA New Zealand Limited, c2005-2021 [cit. 2020-07-20]. Dostupné z: https://www.google.com/url?sa=t&rct=j&q=&esrc=s&source=web&cd=&ved=2ahUKEwj69J_c5dPqAhUBMewKHUKlCAkQFjACegQIAhAB&url=https%3A%2F%2Fwww.hella.co.nz%2Fcontent%2Fshowfile.php%3Fdownloadid%3D840&usg=AOvVaw0rBskjTb0Sxv1Q69ekaHuO
6. LIGHTING THE FUTURE: HIGH PERFORMANCE AUTOMOTIVE HALOGEN BULBS. Hella.com [online]. Dubai, United Arab Emirates: Hella Middle East FZE, c2021 [cit. 2020-07-22]. Dostupné z: https://www.hella.com/hella-ae/assets/media/HMEA_Bulbs_Brochure.pdf
7. XENON HEADLIGHTS. Hella [online]. 4 Hargrave Place, Australia: HELLA Australia, c2021 [cit. 2020-07-29]. Dostupné z: https://www.hella.com/techworld/au/Technical/Automotive-lighting/Xenon-headlights-218/
8. OSCONIQ® P 3737 (3W), GW PULTA1.CM. Osram [online]. Garching, Germany: OSRAM, c2021 [cit. 2020-08-05]. Dostupné z: https://www.osram.com/ecat/OSCONIQ%C2%AE%20P%203737%20(3W)%20GW%20PULTA1.CM/com/en/class_pim_web_catalog_103489/prd_pim_device_4268123/
9. LED HEADLIGHTS. Hella [online]. Peachtree City, USA: HELLA, c2021 [cit. 2020-08-06]. Dostupné z: https://www.hella.com/techworld/us/Technical/Automotive-lighting/LED-headlights-833/#
10. De-icing and ice prevention of automotive headlamps and tail lamps: An investigation of techniques and development of a test method [online]. Stockholm, 2014 [cit. 2020-

08-10]. Dostupné z: http://www.diva-portal.org/smash/get/diva2:718397/FULLTEXT01.pdf. Master of Science Thesis. KTH Materials Science and Engineering.

11. BAEHR, Hans Dieter a Karl STEPHAN. Heat and mass transfer. 2nd edition. Berlin: Springer, 1998. ISBN 3-540-63695-1.
12. KREITH, Frank, R. M. MANGLIK a Mark BOHN. Principles of Heat Transfer [online]. 7th ed. Stamford: Cengage Learning, 2011 [cit. 2021-02-13]. ISBN 0-495-66770-6. Dostupné z: 160592857366.free.fr/joe/ebooks/Mechanical%20Engineering%20Books%20Collection/HEAT%20TRANSFER/Ptinciples%20of%20Heat%20Transfer.pdf
13. INCROPERA, FRANK P., DAVID P. DEWITT, THEODORE L. BERGMAN a ADRIENNE S. LAVINE. Fundamentals of heat and mass transfer [online]. 6th ed. New York: John Wiley, 2007 [cit. 2021-02-14]. ISBN 0-471-45728-0. Dostupné z: https://hyominsite.files.wordpress.com//2015/03/fundamentals-of-heat-and-mass-transfer-6th-edition.pdf
14. Diagram showing how heat transfer. In: VectorStock [online]. Newton, Auckland: VectorStock Media, c2021 [cit. 2021-02-14]. Dostupné z: https://www.vectorstock.com/royalty-free-vector/diagram-showing-how-heat-transfer-vector-27755208
15. Simcenter STAR-CCM+® Documentation: Version 2019.3. Siemens Digital Industries Software [online]. United States: Siemens Product Lifecycle Management Software, c2021 [cit. 2021-02-15]. Dostupné z: https://docs.sw.siemens.com/en-US/product/226870983/doc/PL20191230144651718.userGuide_pdf_2019.3.1/pdf/
16. CCM USER GUIDE: STAR-CD VERSION 4.02. Scribd [online]. San Francisco, CA: Scribd, c2021 [cit. 2021-02-16]. Dostupné z: https://www.scribd.com/doc/193836790/Star-CCM-User-Guide
17. ÇENGEL, Yunus A., Afshin J. GHAJAR a Mehmet KANOGLU. Heat and mass transfer: fundamentals & applications. Fifth edition in SI units. New York: McGraw-Hill Education, 2015. ISBN 9789814595278.
18. Siemens Support: Siemens Digital Industries Software [online]. Munich, Germany: Siemens Product Lifecycle Management Software, c2021 [cit. 2021-02-21]. Dostupné z: https://support.sw.siemens.com/cs-CZ/
19. What is Emissivity? Fluke [online]. Fluke Process Instruments: Fluke Process Instruments, c2021 [cit. 2021-03-31]. Dostupné z: https://www.flukeprocessinstruments.com/en-us/service-and-support/knowledge-center/infrared-technology/what-is-emissivity
20. VAGABOND, John. Black Body Radiation. WordPress.com [online]. San Francisco, United States of America: Physics and Chemistry for IG and A level, 2005, 29 October 2013 [cit. 2020-08-30]. Dostupné z: https://esfsciencenew.wordpress.com/2013/10/29/black-body-radiation/

21. Electromagnetic Spectrum. In: Sapling Learning, Inc. [online]. Austin: Sapling Learning, c2011 - 2021 [cit. 2020-08-30]. Dostupné z: https://sites.google.com/site/chempendix/em-spectrum
22. FRITZSCHE, Hellmut. Wien's law: physics. Britannica [online]. Chicago, IL, United States: Encyclopædia Britannica, c2021 [cit. 2020-09-08]. Dostupné z: https://www.britannica.com/science/Wiens-law
23. HELMENSTINE, PH.D., Anne Marie. Definition and Examples of Latent Heat. ThoughtCo [online]. University of Tennessee at Knoxville: ThoughtCo, c2020, 4 November 2019 [cit. 2020-09-15]. Dostupné z: https://www.thoughtco.com/latent-heat-definition-examples-4177657
24. ENCYCLOPAEDIA BRITANNICA, The Editors of Encyclopaedia Britannica. Latent heat: physics. Britannica [online]. Chicago, IL, United States: Encyclopædia Britannica, c2021 [cit. 2020-09-16]. Dostupné z: https://www.britannica.com/science/latent-heat
25. Heating: Heating Graph. In: Blogger [online]. Austin: Blogger team, c2011 - 2021, August 14 2017 [cit. 2020-08-30]. Dostupné z: http://heatinggondon.blogspot.com/2017/08/heating-graph.html
26. GORAJ, Zdobyslaw. AN OVERVIEW OF THE DEICING AND ANTIICING TECHNOLOGIES WITH PROSPECTS FOR THE FUTURE. ICAS 2004 [online]. Yokohama, Japan: Optimage, c2021 [cit. 2020-10-10]. Dostupné z: http://www.icas.org/ICAS_ARCHIVE/ICAS2004/PAPERS/547.PDF
27. Accumulating Knowledge: De-Ice Boots. In: Cessna Flyer Association [online]. Upland: Cessna Flyer magazine, 2004, 26 September 2018 [cit. 2020-11-10]. Dostupné z: https://www.cessnaflyer.org/maintenance-tech/itemlist/tag/Goodrich%20Deicing.html
28. De-icing. In: Wikipedia: the free encyclopedia [online]. San Francisco (CA): Wikimedia Foundation, 2001 [cit. 2020-11-11]. Dostupné z: https://en.wikipedia.org/wiki/De-icing#Chemical_de-icers
29. AROUSSI, A, S. A. A. Abdul GHANI, A HASSAN a B. S ABDULNOUR. Assessing the Performance of Electrically Heated Windshield. 2002. ISSN 0148-7191. Dostupné z: doi:10.4271/2002-01-0225
30. INGVARSSON, GUSTAF. Assessment of a Thermal DeIcing Solution and Control Methods using Simulations [online]. STOCKHOLM, 2018 [cit. 2020-11-11]. Dostupné z: http://www.diva-portal.se/smash/get/diva2:1290236/FULLTEXT01.pdf. Master of Science Thesis. KTH Materials Science and Engineering. Vedoucí práce Mahmood Reza Khabbazi.
31. *2016 ASHRAE Handbook - Heating, Ventilating, and Air-Conditioning Systems and Equipment*. SI Edition. Atlanta, GA: American Society of Heating, Refrigerating and Air-Conditioning Engineers, Inc. (ASHRAE), 2016. ISBN 9781939200273.
32. File:Makrolon-Sheet transmission.jpg. In: Wikipedia: the free encyclopedia [online]. San Francisco (CA): Wikimedia Foundation, 2001 [cit. 2020-11-15]. Dostupné z: https://commons.wikimedia.org/wiki/File:Makrolon-Sheet_transmission.jpg

33. Temperature coefficient. In: Wikipedia: the free encyclopedia [online]. San Francisco (CA): Wikimedia Foundation, 2001 [cit. 2020-11-23]. Dostupné z: https://en.wikipedia.org/wiki/Temperature_coefficient#Positive_temperature_coefficient_of_resistance
34. SJODIN, Bjorn. What's The Difference Between FEM, FDM, and FVM? Machine Design [online]. Machine Design: Endeavor Business Media, c2021, 18 Apr 2016 [cit. 2021-01-26]. Dostupné z: https://www.machinedesign.com/3d-printing-cad/fea-and-simulation/article/21832072/whats-the-difference-between-fem-fdm-and-fvm
35. Finite Element Method (FEM) vs. Finite Volume Method (FVM) in Field Solvers for Electronics. Cadence [online]. San Jose, CA,: Cadence Design Systems, c2021 [cit. 2021-01-26]. Dostupné z: https://resources.pcb.cadence.com/blog/2020-finite-element-method-fem-vs-finite-volume-method-fvm-in-field-solvers-for-electronics
36. Comparison of finite element and finite volume methods for simulation of natural ventilation in greenhouses. In: Science Direct [online]. Elsevier: Science Direct, c2021, July 2010 [cit. 2021-01-29]. Dostupné z: https://www.sciencedirect.com/science/article/abs/pii/S0168169910000554
37. SRINIVASA, Raju. FVM Literature Review - FDM vs FVM. In: Skill Lync [online]. Thiruvanmiyur: Skill-Lync, c2021 [cit. 2021-01-29]. Dostupné z: https://skill-lync.com/projects/week-9-fvm-literature-review-40
38. ČERNÝ, Ladislav. Scania XT v zimě: Stavba na ledu. In: Auto.cz [online]. CZECH NEWS CENTER a.s: acz, c2001 - 2021, 21. 5. 2018 [cit. 2021-03-14]. Dostupné z: https://www.auto.cz/galerie/profi/60377/scania-xt-v-zime-stavba-na-ledu?foto=33
39. KALOGIROU, Soteris. Thermo-physical Properties of Materials. Oreilly [online]. USA: O'Reilly Media, c2021 [cit. 2021-03-19]. Dostupné z: https://www.oreilly.com/library/view/solar-energy-engineering/9780123972705/xhtml/APP005.html
40. Thermal Resistance. STUG [online]. Victoria, Australia: Stug, c2021 [cit. 2021-03-19]. Dostupné z: http://www.stug.com.au/materials/engineering-plastics-properties/min-max-operating-temperatures.php
41. Plastics: Makrolon® resists heat and attracts innovators. Covestro Solution Center [online]. Covestro: www.covestro.com, c2020 [cit. 2021-03-19]. Dostupné z: https://solutions.covestro.com/en/brands/makrolon
42. Courant number in CFD simulations. *Ideal Simulations* [online]. United Kingdom: IdealSimulations, c2020 [cit. 2021-4-6]. Dostupné z: https://www.idealsimulations.com/resources/courant-number-cfd/

USED SHORTCUTS AND SYMBOLS

Shortcut	Description
CFD	Computational Fluid Dynamics
LED	Light Emitting Diode
HID	High Intensity Discharge
BMW	Bayerische Motoren Werke
PTC	Positive Temperature Coefficient
IR	Infra-Red
CAE	Computational Aided Engineering
IGES	Initial Graphics Exchange Specification
STEP	STandard for Exchange of Product
STL	StereoLithography
EMP	Eulerian Multiphase
VOF	Volume of Fluid
FF	Fluid Film
TF	Thin Film
DMP	Dispersed Multiphase
MMP	Mixture Multiphase
DEM	Discrete Element Method
CAD	Computer-aided design
FEM	Finite element method
FVM	Finite volume method
3D	Three dimensions
UV	Ultraviolet
TF	Thin Film
RSVF	Relative solid volume fraction
PCB	Printed circuit board

Symbol	Unit	Description
P	[W]	Power
U	[V]	Electric potential
Φ_v	[lm]	Luminous flux
q''_x	[W . m^{-2}]	Conductive heat flux
k	[W . m^{-1} . K^{-1}]	Thermal conductivity
ΔT	[K]	Temperature difference
q_x	[W]	Heat rate by conduction
A	[m^2]	Wall of area
q''	[W . m^{-2}]	Convective heat flux
h	[W . m^{-2} . K^{-1}]	Convection heat transfer coefficient
T_s	[K]	Surface temperature
T_∞	[K]	Fluid temperature
E_{Black}	[W . m^{-2}]	Surface emissive power
σ	[W . m^{-2} . K^{-4}]	Stefan-Boltzmann's constant
ε	[-]	Surface emissivity
λ_{Max}	[m]	Peak of the radiated wavelengths
b	[m . K]	Wien's displacement constant
T	[K]	Absolute temperature
L	[J . g^{-1}]	Specific latent heat
Q	[J]	Heat absorbed or released
m	[g]	Mass of substance
u	[m . s^{-1}]	Magnitude of the flow velocity
Δt	[s]	Time step
Δh	[m]	Characteristic size of the mesh cell

APPENDIX A: MACRO CODE (VARIABLE TIME STEP)

This macro code was used as productivity booster. Thanks to this macro huge number of simulations were launched and collected data create the basis of graphs in this master's thesis.

```
// STAR-CCM+ macro: Macro_Test.java

import java.util.*;
import java.io.File;
import java.io.FileInputStream;
import star.common.*;
import star.base.neo.*;
import star.fluidfilm.*;
import star.vis.*;
public class Macro_Test extends StarMacro { //Call the run method

// Function Definition

@Override
public void execute() {
double val = (set initial time step);
String str_val = "";
String str_val_img = "";

Simulation simulation_0 = getActiveSimulation();
String SimName = simulation_0.getPresentationName();
File dir = simulation_0.getSessionDirFile();
String dirS = dir.toString();

for ( int i = 0; i < (set number of simulations) ; i++ ) {
        val = val + (set time step difference);
        str_val = Double.toString(val);
        str_val_img = "(set simulation name)" + str_val;

        Solution solution_0 = simulation_0.getSolution();
        solution_0.clearSolution();

        //Clear solution from previous simulation

        UserFieldFunction userFieldFunction_0 =
        ((UserFieldFunction)
        simulation_0.getFieldFunctionManager().getFunction("Varialble_Val"));
        userFieldFunction_0.setDefinition(str_val);

         //Call user field function
```

```
            Scene scene_0 =
            simulation_0.getSceneManager().getScene("Plots_Fluid_Film_Temperature_Thick
            ness");
            scene_0.initializeAndWait();
            SceneUpdate sceneUpdate_0 = scene_0.getSceneUpdate();
            sceneUpdate_0.setAnimationFilePath(str_val_img);

            //Create scene output file

            simulation_0.getSimulationIterator().runAutomation();
            String output_nameS = SimName + str_val + ".sim"; //
            String filepathS = dirS + "\\" + output_nameS;
            simulation_0.saveState(filepathS);

            //Creates the complete output file path

        }
    }
}

//End Function
```